3-27-2006

Optimizing Biofuel Cell Performance Using a Targeted Mixed Mediator Combination

Jason C. Klar
University of South Florida

Optimizing Biofuel Cell Performance Using a Targeted Mixed Mediator Combination

by

Jason C. Klar

A thesis submitted in partial fulfillment
of the requirements for the degree of
Master of Science in Mechanical Engineering
Department of Mechanical Engineering
College of Engineering
University of South Florida

Major Professor: Stuart Wilkinson, Ph.D.
Muhammad Mustafizur Rahman, Ph.D.
Frank Pyrtle, III, Ph.D.

Date of Approval:
March 27, 2006

Keywords: Microbial fuel cells, mediators, *s. cerevisiae*, yeast, Neutral Red, Methylene Blue, Gastrobots

Dedication

Diantha Mateos

Thank you for three great years, I wish we had more time together

You were my best friend, I love you

I will carry you with me forever

Salud, Amor, Dinero

Acknowledgements

I would like to thank Dr. Wilkinson for giving me the opportunity to work on this project. Thank you for the support and for getting more out of me than I thought I had in myself.

I would like to thank Shawn Applegarth for helping me with my many questions. He helped me most with formatting problems with the thesis. It was good to have someone to ask stupid questions to.

I would like to thank Dr. Pyrtle and Dr. Rahman for reviewing and giving me feedback about my work.

I would like to thank Sue Britten and Shirley Tervort, in the ME department, for their support and encouragement.

I would like to thank Cherine Chehab for correcting all my errors.

I would like to thank Janet Giles for the extension of the deadline.

And finally, I would like to thank my parents for their support.

Table of Contents

List of Tables

List of Figures

List of Symbols

ADH	alcohol dehydrogenase
ADP	adenosine diphosphate
ATP	adenosine triphosphate
CoQ	coenzyme Q, ubiquinone
DAPI	4,6-diamidino-2-phenylindole
DARPA	Defense advanced research project agency
DNA	deoxyribonucleic acid
e.coli	*Escherichia coli*
E'_o	redox potential
FAD	flavine adenine dinucleotide
$FADH_2$	reduced form of flavine adenine dinucleotide
GAPDH	glyceraldehydes-3-phosphate dehydrogenase
GTP	guanosine triphosphate
H^+	hydrogen ion
H_2O_2	hydrogen peroxide
IDH	isocitrate dehydrogenase
KDH	α-ketoglutarate dehydrogenase
$K_3Fe(CN)_6$	potassium ferricyanide
MB	methylene blue
MBH_2	reduced form of methylene blue

MDH	L-malate dehydrogenase
MFC	microbial fuel cell
NAD	nicotinamide adenine dinucleotide
NADH	reduced form of nicotinamide adenine dinucleotide
NADP	nicotinamide adenine dinucleotide phosphate
NR	neutral red
NRH_2	reduced form of neutral red
OCV	open circuit voltage
PDH	pyruvate dehydrogenase
RVC	reticulated vitreous carbon
SDH	succinate dehydrogenase
SHE	saturated hydrogen electrode
SUC/FUM	succinate/fumerate system
TH	thionine

Optimizing Biofuel Cell Performance Using a Targeted Mixed Mediator Combination

Jason C. Klar

ABSTRACT

A study of how mediators interact with the catabolic pathways of microbes was undertaken with a view towards improving the performance of microbial fuel cells. The use of mediators is known to improve the power density in microbial fuel cells, but this work suggests that no single mediator is ideally suited to the task. Instead, a carefully selected mixture of two targeted mediators (Methylene Blue and Neutral Red) might be optimal. To test this hypothesis, a yeast-catalyzed microbial fuel cell was built and empirically evaluated under different mediation conditions while keeping all other parameters constant. The results clearly show that an appropriate mix of the two mediators mentioned could indeed achieve significantly superior performance, in terms of power-density, than when either mediator is used singly. All tests were carried out using the same overall mediator concentration.

Chapter 1 – Background

1.1 Benefits of Biofuels

Biomass is very diverse, ranging from grasses and grains to animal products such as meat or fish. As can be seen from Table 1, the energy density of biomass is generally inferior to fossil fuels, but it can be catabolized into electricity rather than combusted, resulting in a better overall efficiency compared to that of current power plants that use fossil fuels.

The energy density of biomass is vastly superior to leading chemical batteries, offering the promise of extended operation for portable electronic devices such as cell phones, laptop computers, palm-pilots, and GPS systems.

Table 1: Comparison of Energy Densities for Various Sources.

Energy Sources	Type	Energy Density [kcal/g]	Energy Source	Type	Energy Density [kcal/g]
Hydrogen	Gas	33.921	Carbohydrate	D-Glucose	4.061
Gasoline	Octane	11.490			
Animal Fat	Saturated	9.076	Vegetables	Above Ground	0.241
Coal	Coke	7.000			
Meat	Beef (Lean)	2.750	Fruit	Soft & Juicy	0.616
	Chicken	1.500		Citrus	0.372
Insects	Termites	3.500	Primary Batteries	Li/MnO2	0.258
	Grasshoppers	2.000		Zn/MnO2	0.112
Worms	Waxworms	1.811	Secondary Batteries	Ni-MH	0.060
	Mealworms	1.223		Ni-Cd	0.039

1.2 History of Biofuel Cells

As with all branches of science, what we know today about biofuel cells represents the accumulated effort of many. Incredible discoveries and innovations continue to be made today. However, it all had to start with the pioneering work of just a few.

People have known for millennia that some animals have the ability to create electricity. Hieroglyphics from Horapollo dated around 3000 BC depict this ability in Electric Catfish in the Nile, which release a charge as a defense mechanism. Studies of electric fish anatomy eventually led to the discovery that acetylcholine is a vital ingredient to the electrochemical transmission of nerve impulses. Acetylcholine is broken down by the enzyme cholinesterase and all animals have both these biochemicals. Electric eels have a much higher (1000 times) quantity of cholinesterase, which is probably why they can release electric charges up to 600 volts strong [1].

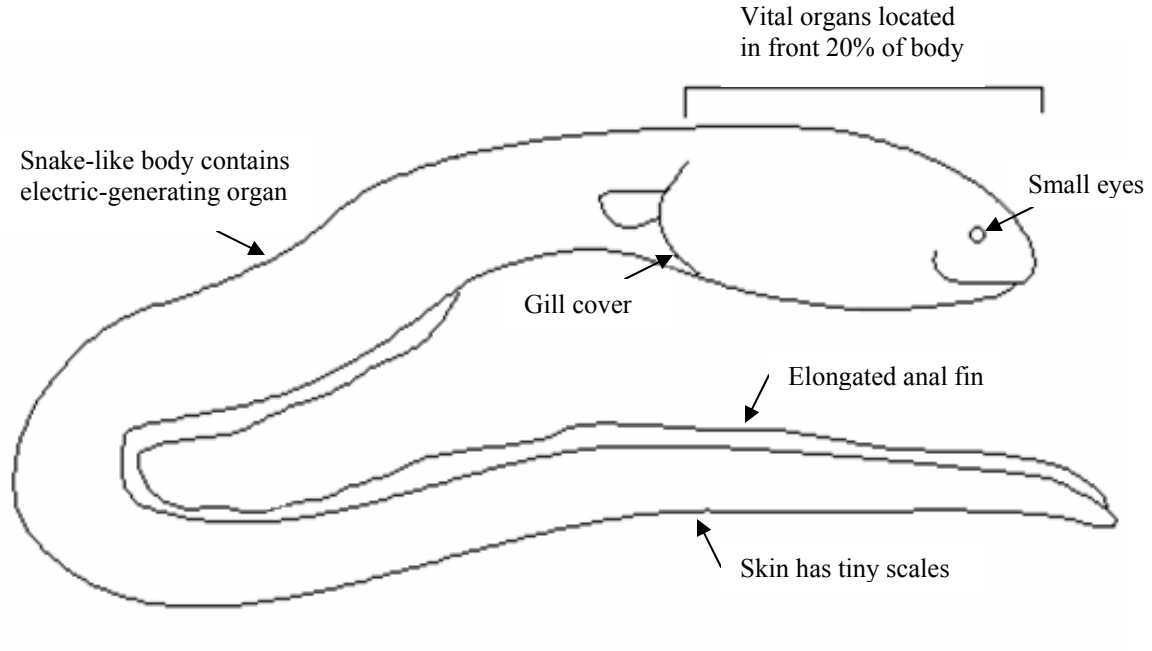

Figure 1: Electric Eel Anatomy.

Luigi Galvani, in 1791, was the first person to show how electricity could be related to biological organisms. He demonstrated this basic link when he applied a voltage to the legs of a frog and observed a muscle spasm in response. Galvani developed a theory of animal electricity, that all animals have an "electrical nerve fluid that reacted to a completed electrical circuit and caused the muscles of even a dead frog to contract"[1]. Galvani's theory was not accepted until Carlo Matteucci was able to prove it in 1831. Matteucci showed, when injured, the frog emitted a small amount of electrical current using a sensitive galvanometer. This injury current didn't require "the aid of metallic or atmospheric electricity". He was not able to detect it in the nervous system, only from the wound itself.

Figure 2: Luigi Galvani.

Michael Cresse Potter, in 1910, demonstrated that organisms (and enzyme extracts) could generate voltage and deliver current. He placed one Platinum electrode in an anaerobic culture containing glucose and yeast (or *Escherichia coli*), and a second in a blank aerobic culture containing no microbes. He recognized intuitively that the electrons came from the degradation of food in the organisms, but little was known about biochemistry or metabolic processes at that time. This is the earliest documented example of a biofuel cell.

In 1931, Barnett Cohen described how a battery of such biofuel cells could produce more than 35 volts. Cohen also used benzoquinone or ferricyanide in the anode

compartment, the first recorded example of the use of chemical mediators to aid in electron transport.

In 1963, Milton J. Allen's pioneering studies of "bacterial electrophysiology" at a number of US institutions, were designed to elucidate the metabolic behavior of *E.coli*. These studies eventually lead to the discovery of the respiratory metabolic apparatus of living organisms (TCA cycle) as shown in Figure 6.

The catabolic generation of electricity from methane and higher hydrocarbons was soon pioneered, along with the earliest enzyme-based and photo-microbial fuel cells. Significant contributions were made by:

- John Davis & Henry Yarborough of the Mobile Co. used *Nocardia* (1962) – also used enzymes
- William van Hess used *Pseudomonas methanica* with CH_4 fuel (1964)
- Hector Videla used *Micrococcus certificans* in Argentina (1972)
- Yahiro used Glucose Oxidase in an enzymatic fuel cell (1964)
- Berk & Cransfield used photosynthetic *Rhodospirillum rubrum* in a photo-microbial fuel cell (1964)

Figure 3: H. Peter Bennetto.

In 1980, H. Peter Bennetto and his 'bioelectrochemistry' group at Kings College, London, contributed greatly in the area of redox mediators as applied to Microbial Fuel Cells (MFCs). The group included: Thurston, Roller, Stirling, Delaney, Mason, and Tanaka (visiting from Japan).

Many fuels have been used in biofuel cells, including: sugars, alcohols, urea, hydrocarbons, sulfide; and even natural biomass such as: molasses, coconut oil, cornhusks, milk whey, fishmeal, plankton, etc. Research in MFC's is an ever-expanding field.

1.3 Fundamentals on How Biofuel Cells Work

The biofuel cell, otherwise known as MFC has been demonstrated [2] as a device that is capable of efficiently converting various food substrates such as carbohydrates, sugars, fats, etc. directly into electricity without combustion, using microorganisms as biocatalysts. The MFC's basic set up consists of an anode and a cathode separated by a proton exchange membrane. The anode contains a biocatalyst (microbe) along with a substrate (sugar) in a buffer solution. As the microbe breaks down the substrate, ions (H^+) and electrons (e^-) are made available within the anode chamber along with some

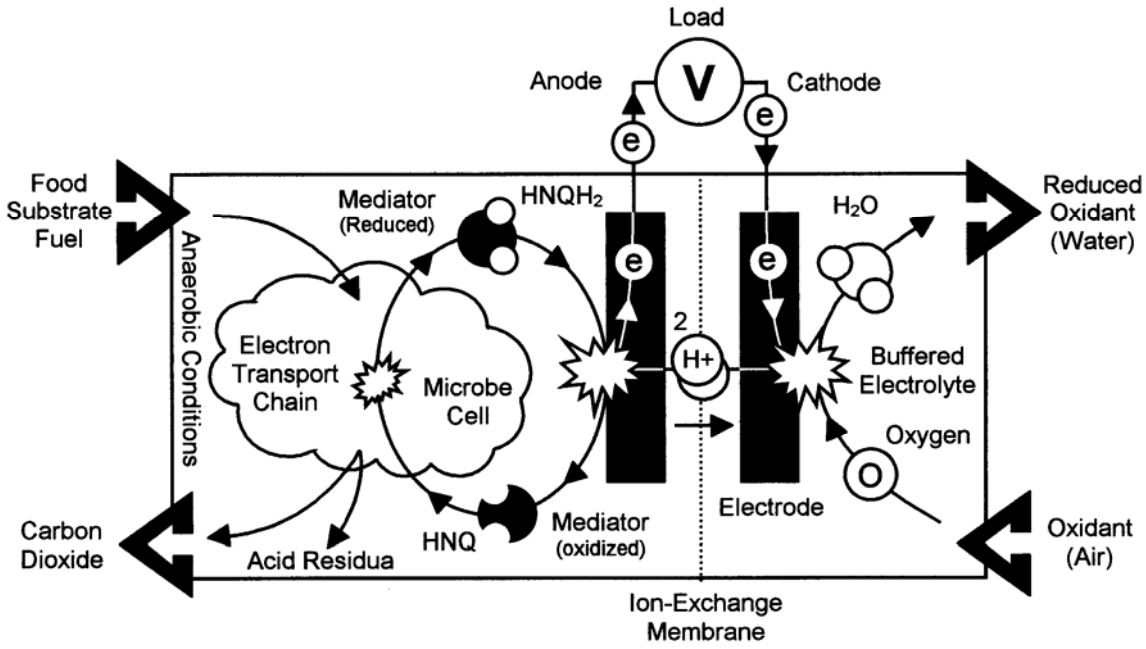

Figure 4: Diagram of a MFC [3].

CO_2. In normal aerobic respiration, the ions and electrons would combine with oxygen to create H_2O. However, this cannot occur due to the anoxic conditions maintained within the anode chamber. Instead, the cathode chamber is enriched with oxygen or some other electron accepter. The cell, in balancing the electric charge, allows the ions to pass through the proton exchange membrane exclusively, while electrons must travel to the cathode via an external circuit, and hence do useful work on a load. Once on the cathode side of the cell; the ions, electrons and oxygen molecules combine to produce H_2O.

1.4 Microbial Fuel Cell Applications

Popular portable consumer electronic devices need light-weight, small, extended operation power sources to replace current battery technology. Due to limited power density, biofuel cells are most likely to appear first as portable battery chargers rather than as direct battery replacements. *Medis Technologies Ltd*. is currently working on an ethanol-fueled charger for the U.S. Army. When combined with MEMS or nano-technologies, biofuel cells may one day become viable no-maintenance, extended-use battery replacements at ambient operating temperatures. The long recharge times associated with batteries would be eliminated by the quick addition of fresh fuel cartridges. Such a lucrative market has attracted a large number of development companies: *Powerzyme*, *Medis Technologies*, *MesoFuel*, *Manhattan Scientifics*, *Lilliputian Systems*, *Angstrom Power*, and *MTI MicroFuel Cells*. Most utilize alcohol fuel, but not all are adopting a bio-catalyzed approach; some use noble metals, extreme pH, and elevated temperatures.

Tiny enzymatic fuel cells are under development which can be surgically implanted into blood vessels, and which utilize blood sugar as fuel. Potential applications include power sources for implantable devices, such as:

- tracking devices
- medical sensors
- telemetry chips
- pacemakers
- data storage

Another potential application for biofuel cells is in *Gastrobots* or food-powered robots, which are autonomous, self-sufficient foraging machines. Their food source can potentially be any biological food. Such systems represent an ideal biomimetic solution to energy demand during long-term start-and-forget missions. *Gastrobots* represent an immense technological challenge, since they must find and ingest complex biomass while tolerating no intervention.

Developed at USF in 2001, by Dr. Stuart Wilkinson, "Gastronome" (a.k.a. Chew-Chew) [4], the world's first food powered robot was built to utilize sugar only as seen on Figure 5. Such a diet has clear advantages for a pioneering prototype, but is not applicable to a self-sufficient gastrobot sustained through foraging [3]. Other gastrobot applications include long-range underwater systems. These aquatic robots would be able to travel great distances, only surfacing to locate position and to deliver data via satellite. The food source for such a device is likely to be plankton or small fish. DARPA is currently funding such a system.

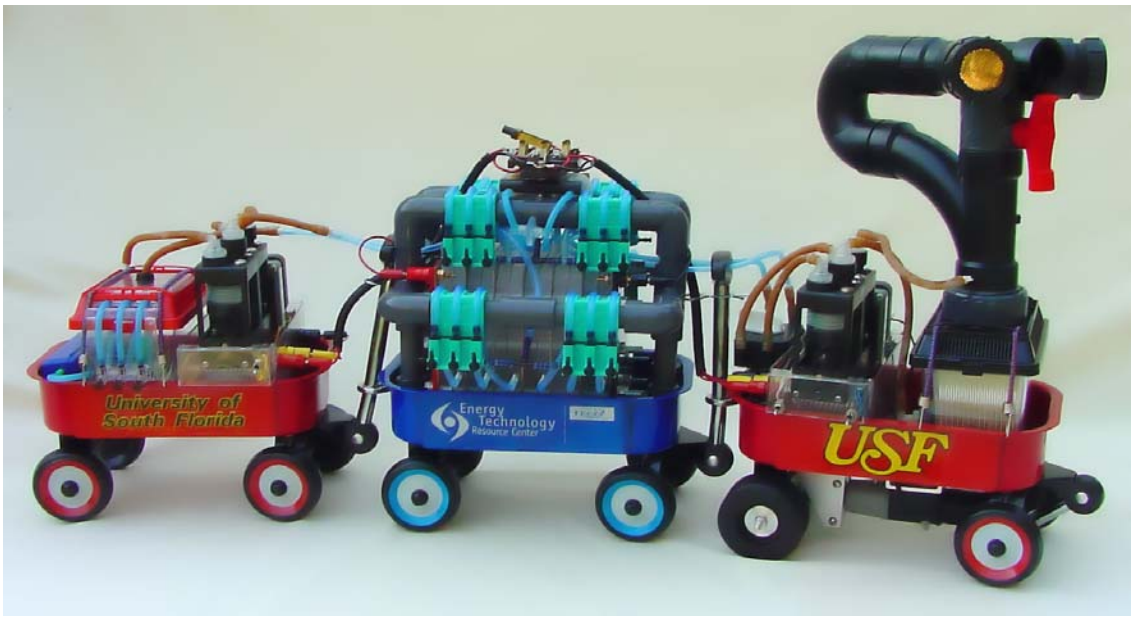

Figure 5: Chew – Chew.

1.5 Why Are Mediators Required?

It is well known that mediators can dramatically improve the performance of whole-cell biofuel cells (or *Microbial Fuel Cells* – MFCs) by acting as an electron shuttle between intracellular reducing centers and an external electrode [5].

Many different mediators have been experimentally studied [6, 7], but relatively little has been reported on why certain mediators work better than others [8, 9]. Mediators are generally used singly, such that only a few examples [10] exist in the literature where combinations of mixed mediators have been employed. The present study represents an early attempt to "tailor" a mixed mediator combination for a specific biocatalyst organism, with the goal of improving MFC performance significantly beyond single mediator levels.

1.6 The Biocatalyst

Since mediators fundamentally work by interacting with the metabolic pathway of the biocatalyst, it was advantageous to choose a well-studied microorganism. Top candidates were *e.coli* and yeast (*saccharomyces cerevisiae*) since both are facultative anaerobic organisms able to switch metabolism from *respiratio*n in the presence of oxygen to *fermentatio*n when anoxic. However, with yeast the metabolic pathway during fermentation is extremely simple, resulting in primary end products of ethanol and CO_2. Yeast was therefore chosen as the biocatalyst since the organism's simple fermentation minimized the number of potential mediator interaction sites, and consequently helped to elucidate the fundamental processes involved. Yeast has been successfully used in MFCs in the past [11, 12].

An additional benefit of using *s.cerevisiae* is that it works well at room temperatures (20 – 25 ºC), unlike *e.coli* that prefers the elevated temperatures associated with its favored enteric habitat. *S.cerevisiae* is also safe and very easy to handle, while being readily available from brewing suppliers.

Chapter 2 – Effects of Mediators

2.1 The Case for Mixed Mediators

Mediators are fundamentally lipophilic chemical electron carriers that are able to pass through the cell walls of microorganisms, and thereby move between intracellular space and the extracellular environment. They are able to assist the microorganisms' metabolism in an anoxic environment by acting as a terminal electron acceptor. Once inside the microbial cell, they are believed to interact with the metabolic process by participating in redox reactions with bioelectrochemical substances such as the pyridine nucleotides (NAD, NADP), flavoproteins, iron-sulfur proteins, quinones, and cytochromes.

Conventional wisdom would indicate the use of a mediator with a low (negative) redox potential, and preferably one with a formal potential close to that of the pyridine nucleotides, as this will maximize the open circuit voltage (OCV) of the MFC and facilitate efficient transfers [13]. However, such mediators may not necessarily generate high power-density because the microbe is generally biased towards a fermentative metabolism due to the absence of oxygen, or any other suitable terminal electron acceptor of sufficiently positive potential in the MFC anode chamber.

Certain mediators are, however, able to act as terminal electron acceptors in the absence of oxygen, and in so doing enable a facultative anaerobe to switch to a nearly

complete respiratory metabolism (*anaerobic respiration*), rather than the fermentation normally demanded by such an anoxic environment. This benefits the MFC performance by enabling more complete oxidation of the fuel, and by generating a larger pool of reducing equivalents. However, to be effective as a terminal electron acceptor the mediator requires a somewhat positive redox potential, preferably one that is close to that of a carrier already in the respiratory chain. By virtue of its positive potential this type of mediator is less able to tap the pool of reduced intermediates.

Clearly the above arguments are mutually exclusive for any single mediator. Instead a mixture of two mediators is called for, one of somewhat positive redox potential to trigger a switch towards anaerobic respiration, combined with one of substantially negative redox potential to exploit the pool of reduced pyridine nucleotides (NADH) present.

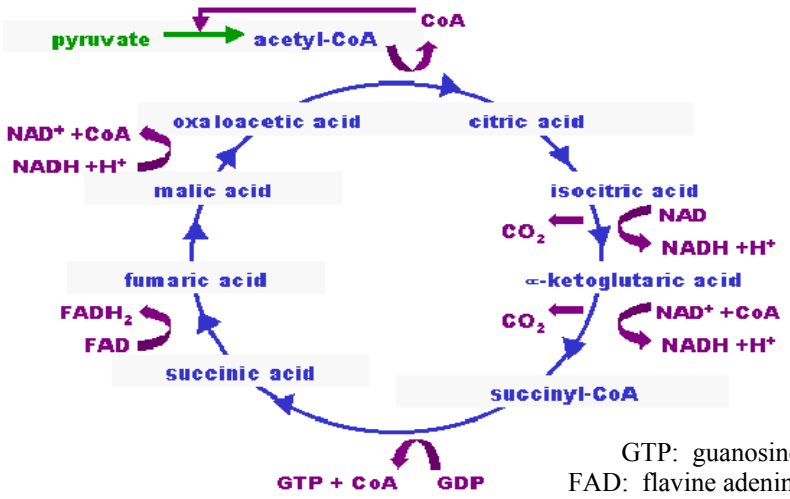

GTP: guanosine triphosphate
FAD: flavine adenine dinucleotide
NAD: nicotinamide adenine dinucleotide

Figure 6: Krebs Cycle (TCA Cycle).

2.2 The Choice of Mixed Mediators

In yeast, as with most other microbes, it is the pyridine nucleotides that constitute the bulk of the reducing equivalents generated. A yeast-catalyzed MFC would therefore

benefit from the presence of one mediator with a redox potential very close to that of NAD (i.e. –0.32 V) to facilitate the direct and efficient transfer of reducing-power from this cofactor.

As for selecting the second mediator, it is clear that the TCA cycle, see Figure 6, cannot become fully established in an anaerobic environment without an electron acceptor of sufficiently positive redox potential. This relates to the step in the cycle where succinate is oxidized to fumarate by succinate dehydrogenase (SDH). The redox potential of the succinate/fumerate (SUC/FUM) system is +0.03 V, which makes it a very weak and unsuitable reductant for NAD or, presumably, any mediator of similarly negative redox potential. Instead, the TCA cycle uses protein-bound FAD as the hydrogen carrier for the SUC/FUM system. Normally the $FADH_2$ generated in the system would feed hydrogen into the respiratory chain via coenzyme Q (CoQ), but in the absence of oxygen this chain leads to a dead-end, thereby precluding the entire respiratory apparatus. However, by providing a mediator with a redox potential close to that of the SUC/FUM system, the $FADH_2$ can become reoxidized and the hydrogen transported out of the microbe via this terminal electron acceptor. For mediator reduction to occur preferentially to CoQ, and thereby

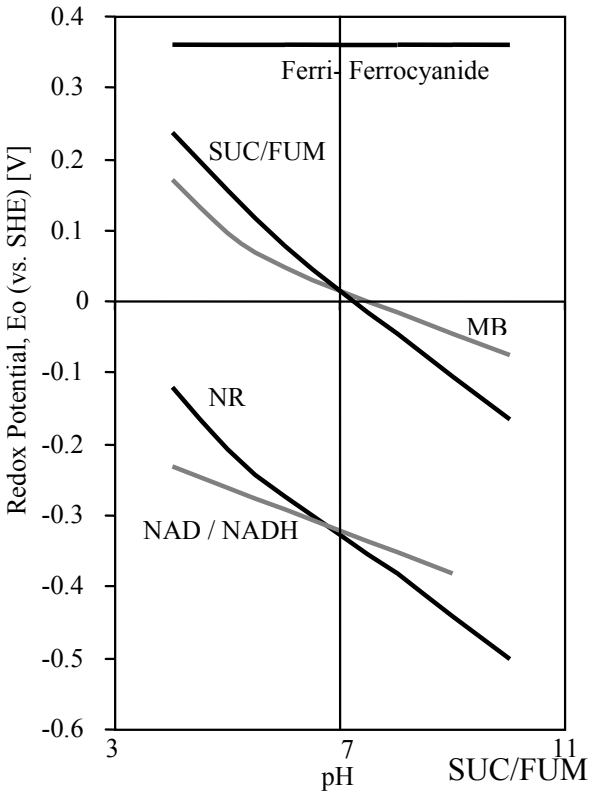

Figure 7: Matching Redox Potentials at pH 7 [14].

maximize OCV, the former should possess a less positive redox potential than the latter (< +0.113 V).

In summary, it would appear that superior performance would result from a yeast-catalyzed MFC if dual mediators are used; one with a redox potential close to -0.32 V and the other with a redox potential close to +0.03 V but less positive than + 0.113 V. Redox potentials are a function of pH, but given that the MFC is to operate at physiological conditions it was only necessary to find two mediators that possessed the necessary potentials at pH 7. Figure 7 shows how *Neutral Red* (NR) at E'_o = -0.325 V clearly represents a near perfect match for NAD at pH 7. Indeed NR has been shown to chemically reduce NAD in vitro [15]. *Methylene Blue* (MB) at E'_o = +0.011 V is a good choice for the second mediator, as complete equilibrium between MB and SUC/FUM has been demonstrated in classical studies [16, 17]. *Thionine* (TH) at E'_o = +0.064 V may be a satisfactory alternate to MB [18], albeit a more expensive one.

2.3 Possible Mediator Interactions

The interactions represented in the following are rather simplistic in that they are based solely on redox potential and the catabolic pathways. The effect of chemical kinetics and polarizations are not considered, nor are interactions that might occur during anabolism. None-the-less these speculations do correspond generally to the broad outcomes observed during experimentation. More detailed experiments are still needed to confirm or deny the hypothesis presented in the following. How deleterious mediators are to living cells is not clear, but at the very least, robbing a cell of reducing power that would normally be employed in ATP synthesis can only be considered antagonistic.

2.3.1 Performance Using NR Only

Normal yeast fermentation of glucose uses NAD as the sole electron carrier, acting as a reducing coenzyme for glyceraldehyde-3-phosphate dehydrogenase (GAPDH) and as an oxidizing coenzyme for alcohol dehydrogenase (ADH) in balanced reactions requiring no external hydrogen acceptor. Two NADH are thus generated for each mole of glucose fermented. The addition of NR is unlikely to precipitate any switch to anaerobic respiration (given its low redox potential), and so it will most likely interact with the fermentative pathway. Figure 8 shows how this interaction could occur in three possible ways, denoted by n = 0, 1 or 2.

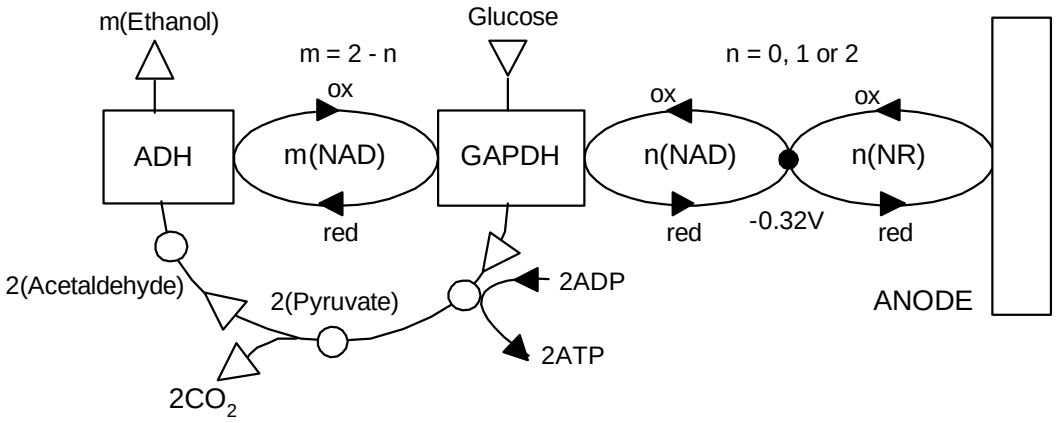

Figure 8: Yeast Fermentation Pathway With NR Only.

It is quite possible that at any given moment or location in the MFC, no oxidized NR has permeated inside a particular yeast cell. This scenario is indicated by n = 0, and fermentation will proceed as normal with the production of two mol of ethanol and no contribution to the MFC output. The case where n = 1 suggests that some intracellular oxidized NR is available and consequently the reduced NADH is partly reoxidized by ADH and partly by the NR. This latter case will only generate one mol of ethanol per mol of glucose, leaving one mol of acetaldehyde unoxidized and providing a limited

flow of reducing power via the anode. Finally, when n = 2 no ethanol is produced and the entire reducing power of 2 mol NAD per mole of glucose is exchanged with the anode. This scenario is most likely to occur under conditions of high mediator concentration where the yeast cells are saturated in NR and the chemical kinetics are not seriously rate limiting. The greatest MFC output is anticipated under these circumstances, but it is unclear whether a corresponding buildup of acetaldehyde will occur or if the yeast will terminate its metabolic pathway at pyruvate.

The anodic half reaction for n = 2 becomes:

$$\text{Glucose} + 2\text{ADP} + 2\text{NR} \rightarrow 2\text{Acetaldehyde} + 2\text{ATP} + 2\text{NRH}_2 + 2\text{CO}_2$$

The free energy is expressed by $\Delta G'_o = eF\Delta E'_o$, where eF = 46 kcal/V for the transfer of two electrons (e = 2). If an oxygen cathode ($E'_o = +0.82$ V) is employed in the MFC the $2NRH_2$ represents a free energy of 2 [46 (0.82 + 0.32)] = 105 kcal per mol of glucose or 15% energy efficiency (given that the free energy of oxidation for glucose is 686 kcal/mol).

2.3.2 Performance Using MB Only

In the presence of a suitable terminal hydrogen acceptor such as MB, yeast is likely to switch to anaerobic respiration. This initially involves the Embden-Meyerhof pathway from glucose to pyruvate, which includes one NAD reduction. Pyruvate is then oxidized to acetyl-CoA by the PDH complex with one more NAD reduction, after which the TCA cycle adds a further three NAD reductions. These latter three are associated with the α-ketoglutarate dehydrogenase (KDH) complex, L-malate dehydrogenase (MDH) and NAD-specific isocitrate dehydrogenase (IDH). With two mol of pyruvate generated and two turns of the TCA cycle needed to completely oxidize a mole of glucose, ten NADH are generated per mole of glucose by respiring yeast.

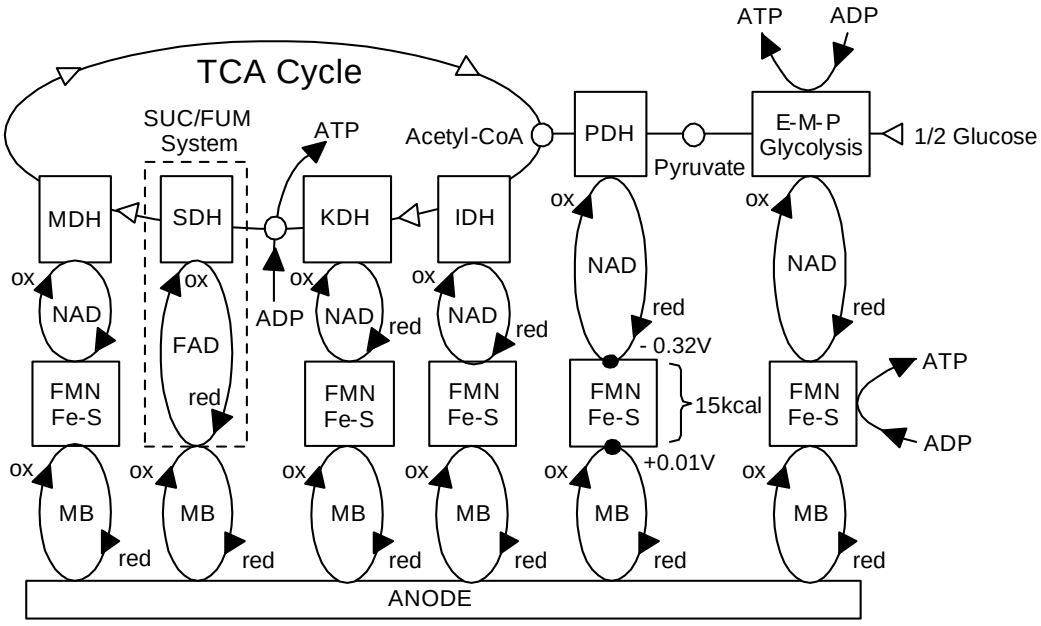

Figure 9: Yeast Anaerobic Respiration With MB Only.

As depicted in Figure 9, the primary role of MB is as a terminal hydrogen acceptor ideally matched to the redox potential of the SUC/FUM system. MB thereby acts as a surrogate for coenzyme Q and enables a switch to anaerobic respiration. Yeast

respiration clearly offers five times the NADH yield as compared with fermentation, but since MB is only a weak reductant for NADH it is not well suited to tapping these reducing equivalents directly. The yeast must employ the flavoproteins (FMN) and iron-sulphur proteins (Fe-S) of its normal respiratory chain to affect the reoxidation of NADH. The aforementioned proteins allow the coupling of NAD/NADH at -0.32 V to MB/MBH_2 at +0.011 V via a series of reducing steps that corresponds to a free energy of 15 kcal/mol of NAD. Given that ten NADH are produced per mol of glucose, this NAD/MB coupling apparatus represents an MFC output energy loss of 150 kcal/mol of glucose. The yeast may, however, benefit since it is able to generate ATP from this coupling site in the same way as it does when coupling NAD to CoQ in normal aerobic respiration.

The anodic half reaction for the case of MB only becomes:

$$\text{Glucose} + 6H_2O + 14ADP + 12MB \rightarrow 14ATP + 12MBH_2 + 6CO_2$$

In this case 2ATP is generated during glycolysis, 2ATP by the TCA cycle itself, and 10ATP by electron-transport phosphorylation. When employing an oxygen cathode in the MFC, the $12MBH_2$ represents a free energy of 12 [46 (0.82 - 0.011)] = 447 kcal per mol of glucose or 65% energy efficiency.

2.3.3 Performance Using Both MB and NR

As can be seen in Figure 10, the effect of including both MB and NR is to eliminate the need for the FMN and Fe-S, as NR and NAD are able to couple directly. This deprives the yeast of 10ATP but makes this extra energy available to the MFC via the oxidation of NR at the anode.

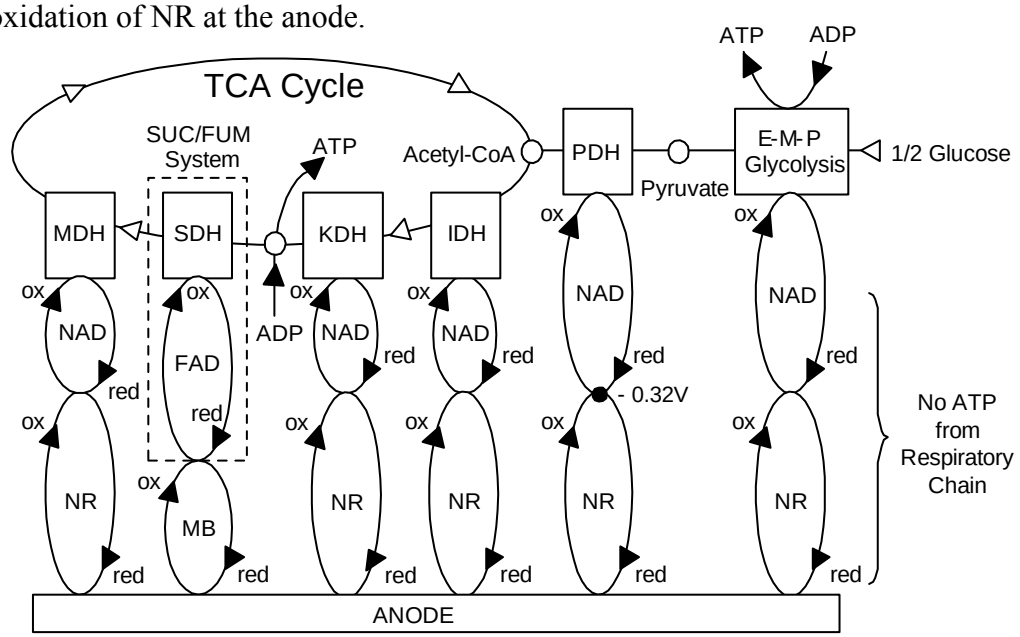

Figure 10: Yeast Anaerobic Respiration With NR and MB.

The anodic half reaction for mixed MB and NR becomes:

$$\text{Glucose} + 6H_2O + 4ADP + 2MB + 10NR \rightarrow 4ATP + 2MBH_2 + 10NRH_2 + 6CO_2$$

In this case 2ATP is generated during glycolysis and 2ATP by the TCA cycle itself. When employing an oxygen cathode in the MFC, the $2MBH_2 + 10NRH_2$ represents a free energy of 2 [46 (0.82 - 0.011)] + 10 [46 (0.82 + 0.32)] = 599 kcal per mol of glucose or 87% energy efficiency.

Chapter 3 – Breakdown of Test Experiment

3.1 Apparatus & Methods

A small desktop apparatus was built to test the hypothesis that a yeast-catalyzed MFC will perform better under mixed mediation than when mediators are used singly at the same overall mediator concentration. Apart from mediation, all other test parameters were kept constant throughout the main experimental program.

Figure 11: Entire Apparatus.

3.1.1 Mechanical Components of the Fuel Cell

- Compartments: Annular virgin-grade PTFE (Teflon™)
- End Plates: Square transparent Plexiglas™
- Seals: Silicon rubber o-rings
- Electrodes: Reticulated vitreous carbon (RVC), 100 pores per inch
- Membrane: Nafion™ 115
- Current Collector: Square carbon felt washer
- Hardware: All Stainless Steel bolts and nuts

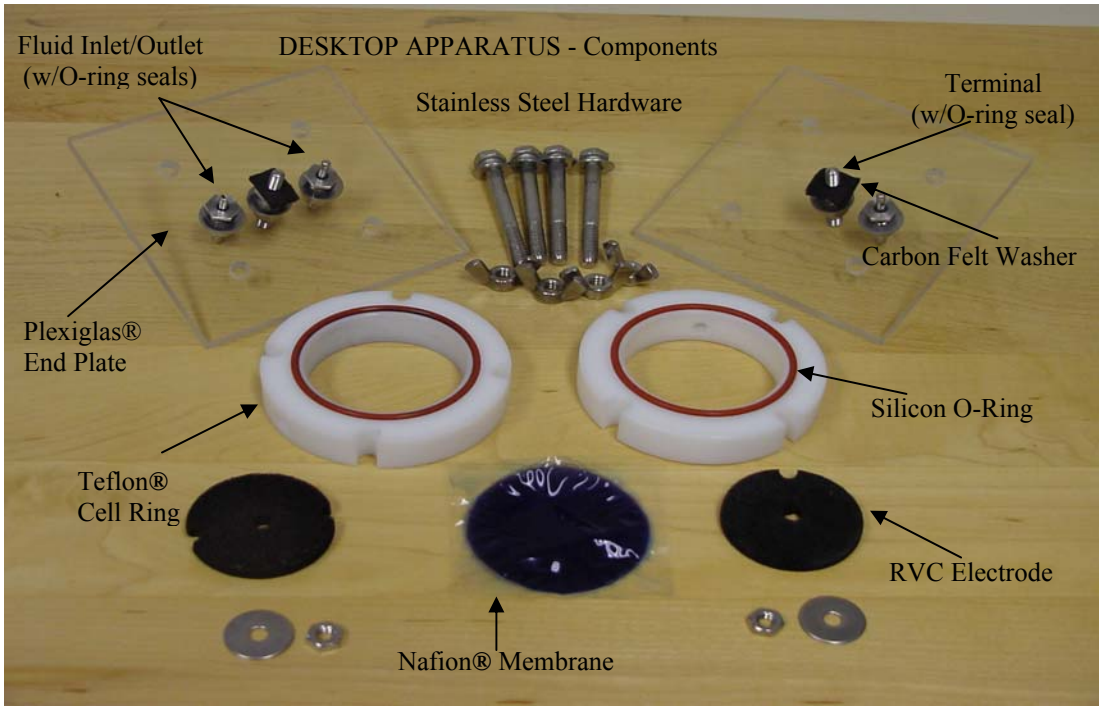

Figure 12: Mechanical Components of the Fuel Cell.

3.1.2 Physical Dimensions of the Fuel Cell

- Compartment Volumes: 32 mL each (both anode and cathode).
- Electrodes: Circular, 4.22 cm diameter x 0.584 cm thick.
- Electrode Geometric Area: 30 cm^2 of exposed RVC (as used in power-density calculations).
- Membrane Exposed Area: Circular, 5 cm diameter.

3.1.3 Assembly of Fuel Cell Apparatus

The chambers for the anode and cathode were contained by the annular virgin-grade PTFE (Teflon™) with a Nafion™ membrane sandwiched between them. Leakage was prevented between chambers and membrane using Silicon rubber o-rings. A small amount of silicon grease was used to hold the o-rings in place during assembly. RVC was chosen for the electrodes due to it's conductive properties, its biocompatibility, and

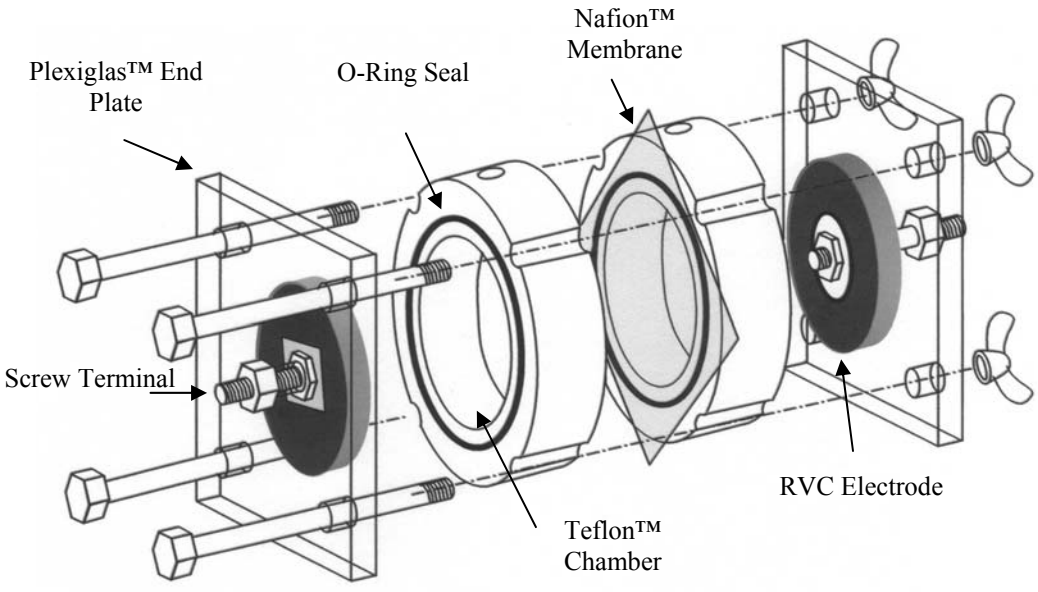

Figure 13: Microbial Fuel Cell (Gas Ports and External Plumbing Not Shown).

high surface area to volume ratio. Stainless steel hardware that was attached to the electrodes protruded through the endplates, thereby making electrical screw terminals. A carbon felt washer was used on both electrodes to cushion this friable material during clamping and to act as current collectors. Each electrode was positioned within the chamber equidistant from the Nafion™ membrane and the Plexiglas™ end plate. A different membrane was used for each of the four mediation conditions of: no mediator, Methylene Blue, Neutral Red, and mixed Methylene Blue with Neutral Red. This step ensured that there would not be any MB contaminating the NR test or vice versa. The endplates were square transparent Plexiglas™ to create a stable base and to allow observation of the internal bioelectrochemical components. The entire apparatus was held together and easily disassembled using four bolts with wing nuts.

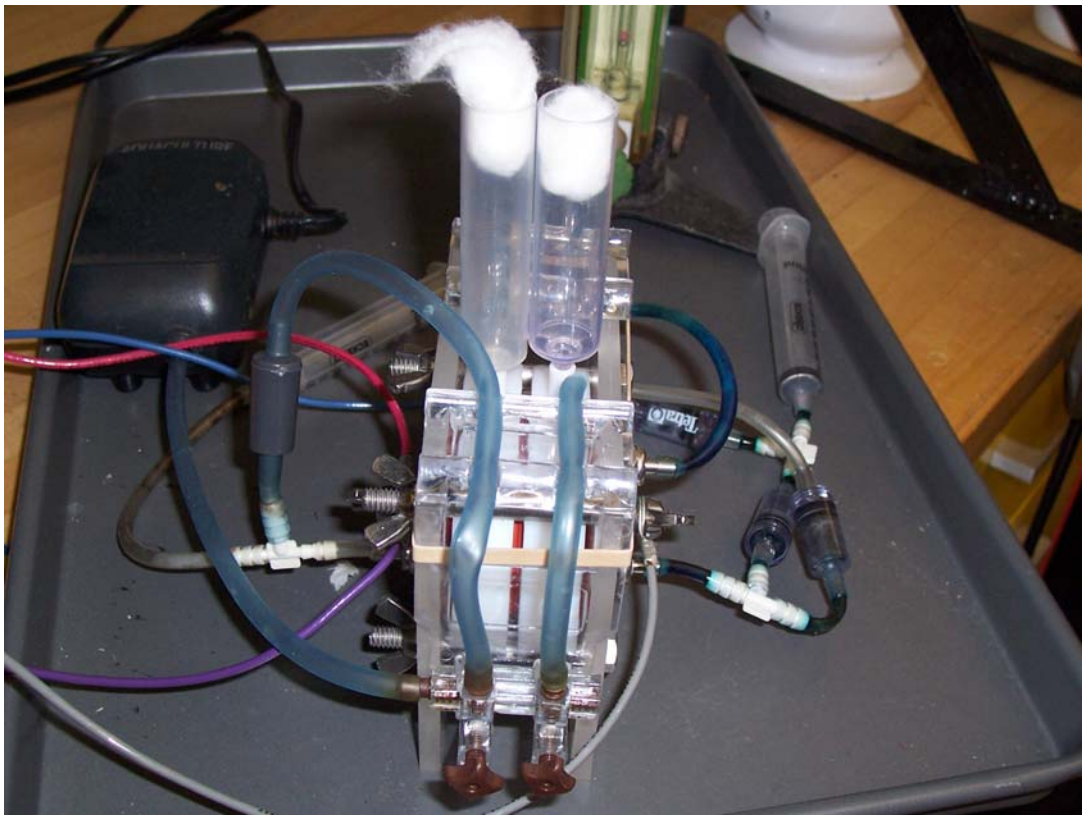

Figure 14: Side View of Fuel Cell (Cathode on Left, Anode on Right).

3.1.4 Wiring of the Experiment

The MFC's terminals were connected directly across two resistance decade boxes in series. The voltage across these resistance decade boxes was monitored using a Fluke® Data Bucket 2635A precision multimeter and logger. The logger recorded voltage at precisely five-second intervals. Data was also sent to a P.C. running Fluke® Hydra Logger™ and Trend Link™ software to further monitor the voltage. The wire used in the apparatus was 12-AWG copper. A knife switch was included in the circuit to switch between open-circuit and loaded modes of operation.

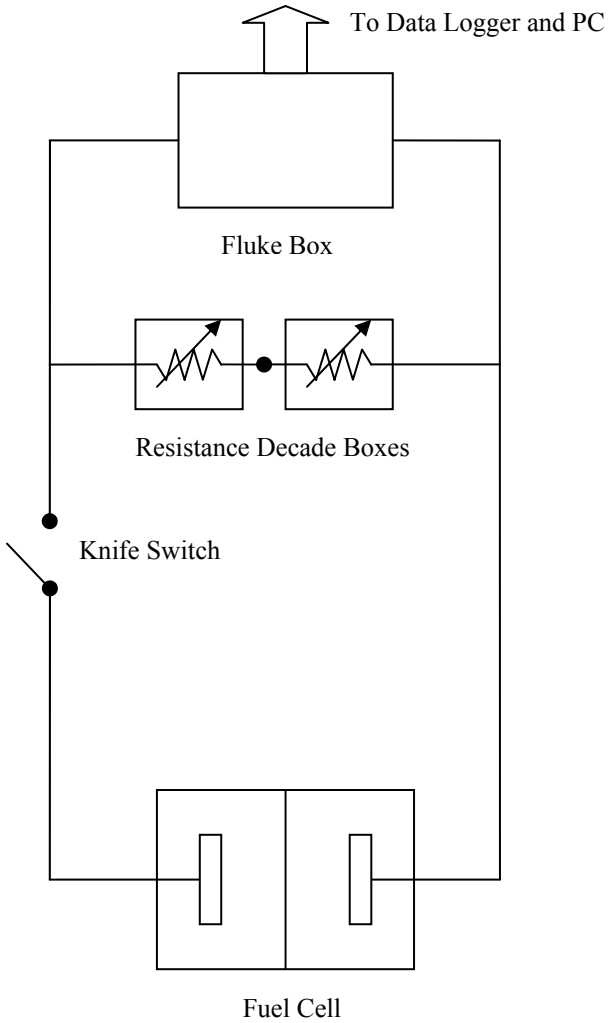

Figure 15: Schematic Representation of Wiring of the Experiment.

3.1.5 Electrical Components

- Real-time Monitoring: P.C. running Fluke® Hydra Logger™ and Trend Link™ software.
- Circuit Control: Knife switch to select between open-circuit or loaded condition.
- Electrical Measurements: Fluke® Data Bucket 2635A precision multimeter and logger.
- Electrical Loads: Resistance decade boxes using 53 values ranging from 1,000,080 Ω down to10 Ω.

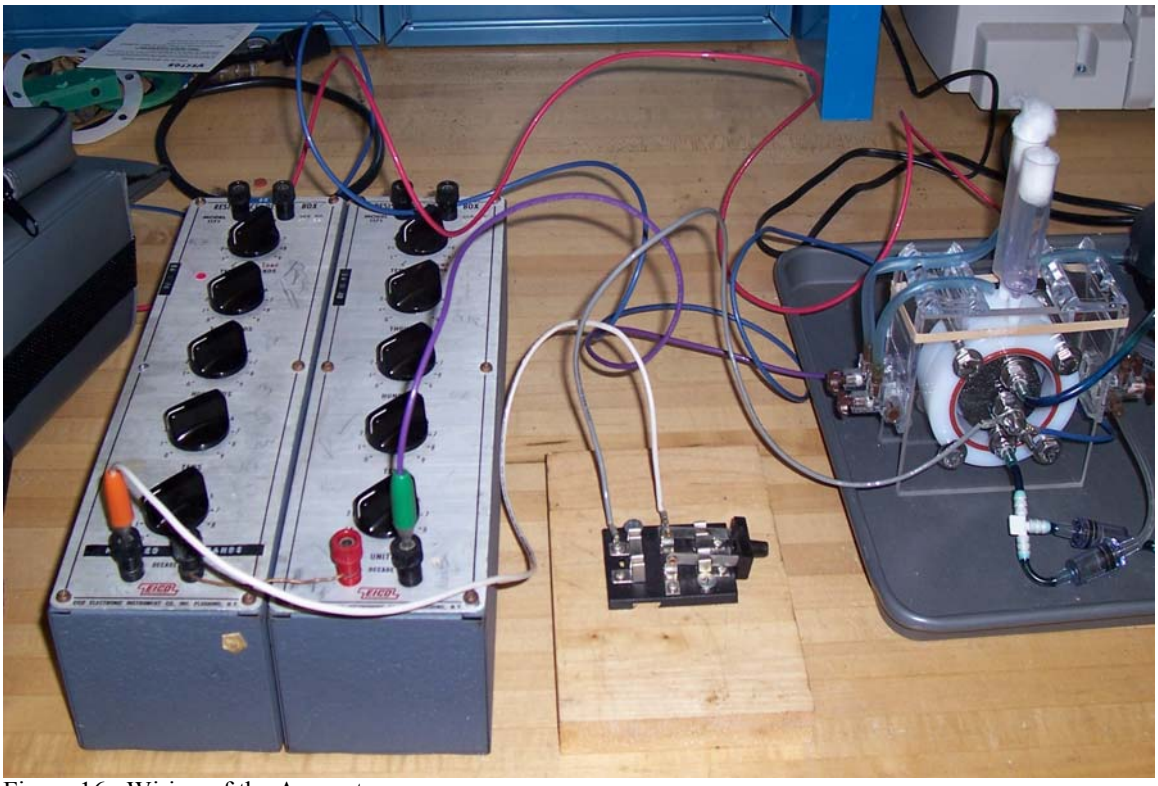

Figure 16: Wiring of the Apparatus.

3.2 Sequence of Resistors

Output voltage data from the MFC was collected at different loads. These loads were provided by two electrical resistance decade boxes wired in series. Each decade box had five selector switches, which were used to adjust the total resistance of the box. All five of these switches were used in the case of the first box, while only one switch was utilized on the second box. At the outset of the test, the first box had all its switches set to their maximum values (marked 9 in each case). This resulted in a total resistance for the first box of 999,990 Ω (i.e. $9 \times 10^5 + 9 \times 10^4 + 9 \times 10^3 + 9 \times 10^2 + 9 \times 10^1$ Ω). The second box used only one switch, which was set to just 90 Ω (i.e. 9×10^1 Ω). The remaining four switches on the second box were set to 0Ω or short circuit. Since the two boxes were wired in series the initial resistance across the MFC was 1,000,080 Ω (i.e. 999,990 Ω + 90 Ω). During MFC testing the load resistance was incrementally reduced by switching just one switch at a time, the sequence was as follows: The resistance decade box was first started at a maximum value of 1,000,080 Ω then proceeded to drop at 100,000 Ω increments until it reached 100,080 Ω, see curve 1 on Figure 18. At 100,080 Ω, it dropped at 10,000 Ω increments until it reached 10,080 Ω, see curve 2 on Figure 18. At 10,080 Ω, it dropped at 1,000 Ω increments until it

Figure 17: Two Resistance Decade Boxes Wired in Series.

reached 1,080 Ω, see curve 3 on Figure 18. At 1,080 Ω, it dropped at 100 Ω increments until it reached 180 Ω, see curve 4 on Figure 18. At 180 Ω, it dropped 10 Ω increments until it finally reached 10 Ω, see curve 5 in Figure 18.

The reason 90 Ω was added using a second resistance decade box was because the slope of the power-resistance curve changed rapidly so more data points needed to be obtained between 100 and 200 Ω to give a smoother representation of the graph, see Appendix 9.

Load resistance was changed consistently using the decade boxes and voltage was recorded once the value stabilized each time. Once resistance and voltage data had been collected, current and power could be calculated and tabulated.

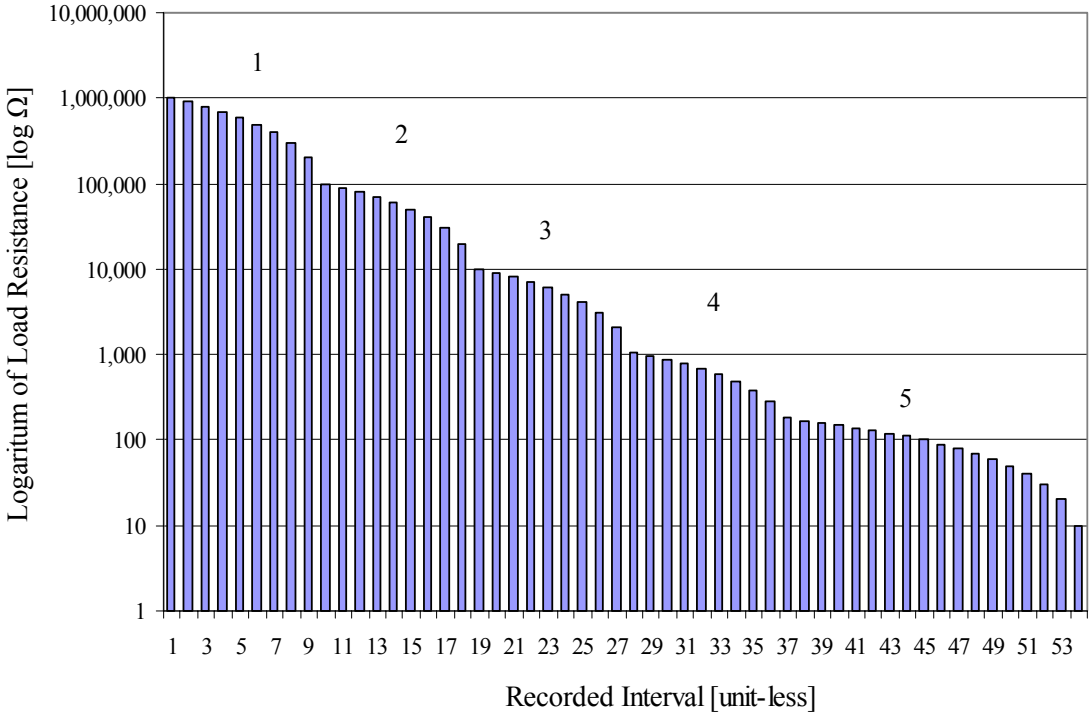

Figure 18: Selection Order of Decade Box Resistances.

3.3 Fluid Systems

3.3.1 Gas Systems

An air pump was used to percolate air through the aquarium air-line tubing which was attached to the cathode to stimulate mixing and to introduce more oxygen in the catholyte. The anolyte was agitated using a constant flow of 99.9999% N_2 using non-permeable Tygon® tubing and thereby purged of O_2. A flow meter was employed to maintain a constant flow of the Nitrogen; however, different flow rates were explored to maximize the fuel cell's effectiveness. It was noticed that too much flow of Nitrogen was detrimental to the performance of the MFC, presumably because the gas pockets prevented adequate contact between electroactive components and the electrode surface.

3.3.2 Plumbing Harnesses

The anode's plumbing harness included a series of check valves, Tygon® tubing, tubing tees, and a syringe. Plunging of the syringe would stir the contents of the MFC and give the anolyte more uniformity. It was noted that mixing of the anode using this method after the fuel cell was running was detrimental to the performance of the MFC, presumably because it dislodged the microbes (yeast) from their locations on the electrode surface and thereby hindered electron exchange. The syringe plunging system was invaluable in drawing the anolyte components into the chamber initially and was also beneficial in the cleanup process by evacuating most of the liquid before having to unbolt it. Three entire anode harnesses were created, one for each: no mediator which was later

converted into NR only, MB only, and mixed MB with NR. This was a precautionary measure to eliminate contamination between the tests.

The cathode's air harness differed from the anode's because it used aquarium air-line tubing instead of the expensive Tygon® tubing. The cathode had atmospheric air pumped into it, so the non-permeable tubing was not necessary. The cathode also had a syringe and a check valve system that was utilized during filling, mixing and cleanup processes.

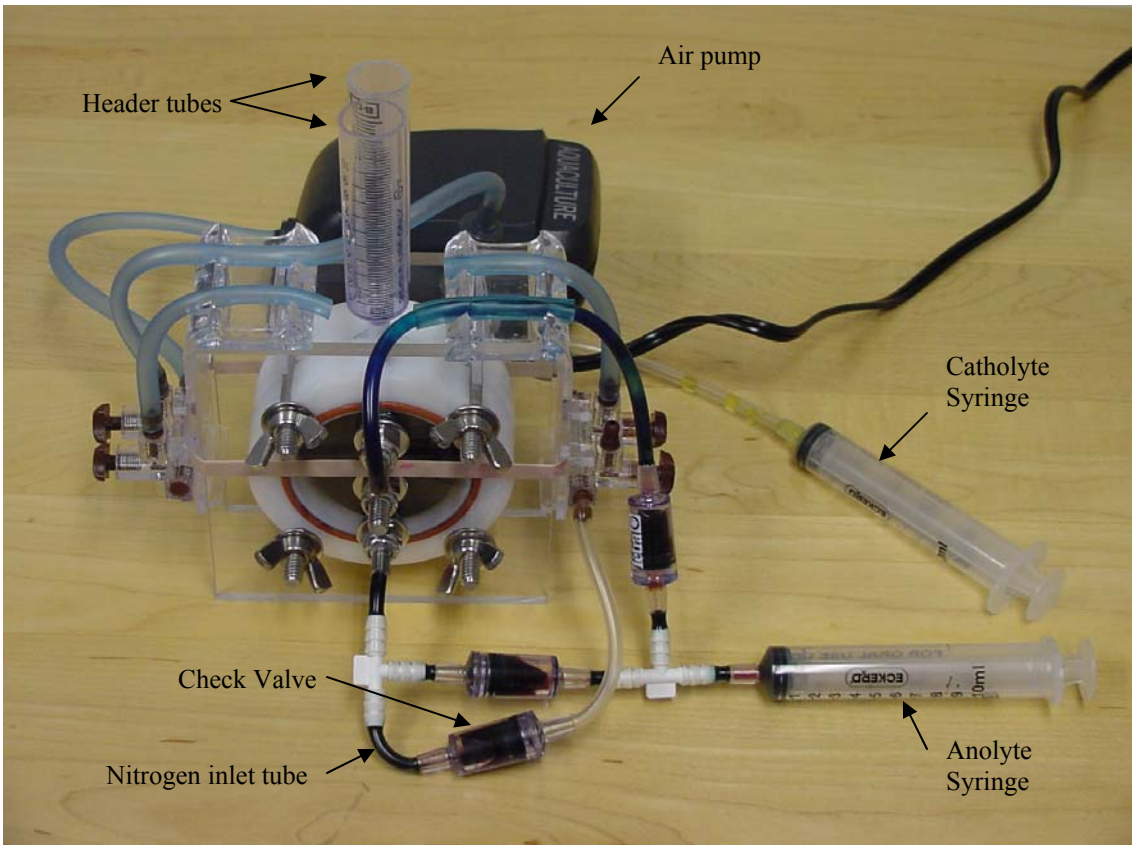

Figure 19: Fuel Cell Showing Plumbing Harnesses (Anode in front, Cathode in back).

3.4 Bioelectrochemical Components

- Buffer: 0.1 M Phosphate (mixed potassium & sodium) @ pH 7.
- Substrate (final concentration in anolyte): 50 mM dextrose.
- Biocatalyst: 5/8 g dry wt. (25 mg/mL of anolyte, 10^{10}-10^{11} cells) *S. cereivisiae* (Red Star - Pasteur Champagne, active dry wine yeast, Lesaffre Corp).
- Mediators: Methylene Blue (Riedel-deHaen 32723 > 98%), Neutral Red (SIGMA N7005 > 96%).
- Mediation (final concentration in anolyte): 1 mM.
- Anolyte: Substrate + Biocatalyst + Mediator, in 0.1 M Phosphate Buffer, pH 7.
- Catholyte: 0.1 M Potassium Ferricyanide, $K_3Fe(CN)_6$ in 0.1 M Phosphate Buffer, pH 7.

3.5 Pre-Mixing of Solutions

3.5.1 Buffer Solution

A 0.1M Phosphate buffer at pH 7 was created using 200mL distilled water and a combination of 1.0534 grams of Potassium Phosphate (Monobasic) and 1.74 grams Sodium Phosphate in precise amounts. Then the pH of the buffer was tested using a digital pH meter. Final minor adjustments were then made as follows: if the pH was too acidic, Sodium Phosphate was added and if the pH was too basic, Potassium Phosphate was added to get a desirable pH of 7 ± 0.01. This buffer was used to prepare both the anolyte and catholyte.

3.5.2 Substrate Solution

20 mL of sugar solution was prepared prior to each test, although only 17 mL was actually added to the anode chamber to achieve the correct concentration. To prepare the sugar solution 0.339 grams of dextrose was added to 20mL of buffer solution to create a concentration of 94 mM.

3.5.3 Catholyte Solution

A 0.1M Potassium Ferricyanide solution was prepared by adding 1.054 grams of the reddish-orange crystals to 32 mL of buffer solution. Swirling was required to ensure that the Ferricyande had completely dissolved.

3.5.4 Methylene Blue Mediator Solution

Methylene Blue (MB) has a formula weight of 319.86 g/mol. A batch of this mediator solution was prepared by adding 0.0512 grams of MB to 50 mL of buffer to create a concentration of 3.2 mM.

3.5.5 Neutral Red Mediator Solution

Neutral Red (NR) has a formula weight of 288.78 g/mol. A batch of this mediator solution was prepared by adding 0.0462 grams of NR to 50 mL of buffer to create a concentration of 3.2 mM.

Each of these solutions were swirled until all solid material had fully dissolved. Excessive agitation was avoided so as not to oxygenate these solutions. Once all solutions had been prepared, testing was commenced as soon as possible because the yeast will become less effective over time.

3.6 Adding the Solutions to the Fuel Cell

Prior to collecting data, the MFC was prepared by adding ingredient solutions.

1. 10 mL of 0.1 M Ferricyanide was added into the top of the cathode using a syringe. Different syringes were used for dispensing each ingredient so as to avoid cross contamination, especially since ferricyanide is toxic to yeast.
2. 10 mL of 94 mM sugar solution was added into the top of the anode using a second syringe.
3. 10 mL more of 0.1 M Ferricyanide was added into the top of the cathode using the cathode syringe.
4. 7 mL of 94 mM sugar solution was added into the anode using the anode syringe, completing the desired amount of sugar solution.
5. 12 mL of 0.1 M Ferricyanide was added into the top of the cathode using the cathode syringe, completely filling the cathode.
6. 5 mL of yeast was added into the anode, using the anode syringe.
7. 10 mL of 3.2 mM mediated buffer was added into the anode creating a final concentration of 1.0 mM mediated buffer, completely filling the anode. This was

the case when using MB or NR exclusively. For the case of mixed mediators, 5 mL of MB together with 5 mL of NR were both added.

Filling the chambers slowly and evenly was important in eliminating bending of the membrane, which, in severe cases can lead to shorting of the electrodes. Since 32 mL of the various solutions were added to both the anode and the cathode chambers, their height levels were the same. This was checked visually through the plexiglas endplates to confirm a successful fill procedure. At this point, all solutions have been added to the fuel cell.

3.7 MFC Capping

Having added all the solutions to the MFC, the two chambers were each capped off using a small header tank (made from syringe bodies). They were held in place by inserting their nozzle ends into a small hole on top of the anode and cathode chambers. These holes were needed to allow gases to escape. A cotton ball was placed on the top of each header tank to catch any anolyte/catholyte that splashed up through the small holes due to the force of escaping gases. (N_2 for the anode, pumped air for the cathode)

3.8 Startup

To start the experiment, the Fluke® Hydra Logger™ and Trend Link™ programs were activated. Once started, values for voltage were witnessed on the P.C. monitor using the Hydra Logger™ program, and also directly displayed on the digital output for

the Fluke Data Bucket 2635A Multimeter. The air pump was then turned on to aerate the cathode and to maintain an elevated oxygen mixture. The Nitrogen tank was then turned on to agitate the anolyte and purge oxygen. Flow was adjusted to a constant flow rate. The voltage would then climb until it reached a peak; this peak value represented the Open Circuit Voltage (OCV). Starting at the largest resistance, the load was reduced one increment at a time, while recording voltage at each increment. This procedure ensured only light current draw initially; heavy current draws tend to deplete the charge within the cell faster than the microbes can maintain it.

3.9 Cleanup

After data was collected, it was important to thoroughly clean the apparatus prior to commencing the next test. This involved the following steps:

- Electrode Preparation: Washed in 70% ethyl alcohol, then rinsed in distilled water, then washed in muriatic acid (20 mL 20° Baume diluted in 125 mL distilled water), then rinsed in distilled water and air dried. This procedure was very important because yeast cells can freely flow through these open pores and sometimes become stuck. This can result in clogging, which restricts the flow of anolyte through the electrode. Also the mediator dyes used can stain the electrodes.
- Hardware Preparation: Biofuel cell structure was thoroughly washed using alcohol and distilled water. A new membrane, external tubing, valves, o-rings and syringes were used for each mediator.

Chapter 4 – Experimental Results

The results of the experimental program are shown in Figure 20. It should be noted that these results are with respect to a Ferricyanide cathode (E'_o = +0.36 V), and that as a consequence the voltage and power-density data are lower than might be expected with an oxygen cathode (E'_o = +0.82 V).

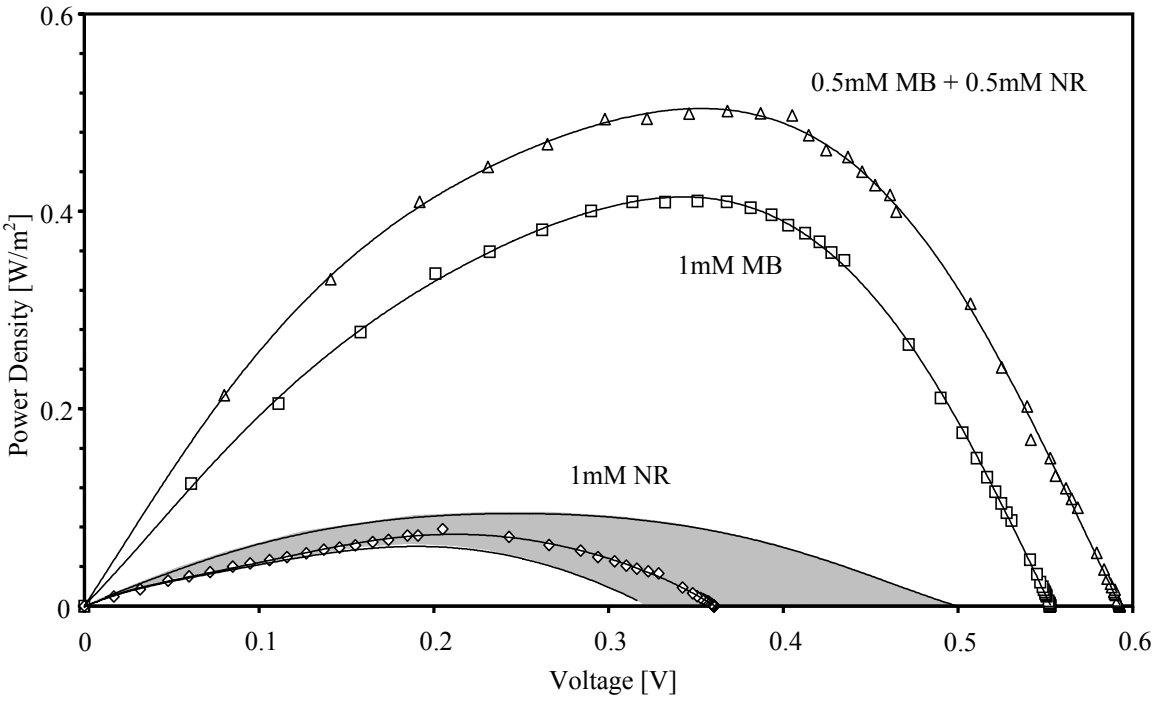

Figure 20: Performance Results Using Single and Mixed Mediation.

As previously predicted, the results obtained when NR was used alone were rather poor (in terms of peak power-density). It also proved to be very difficult to obtain consistent results, such that no performance curves were exactly alike, even after repeating the same NR experiment eight times. Figure 20 shows a typical performance

curve for NR bounded by a shaded region that represents the spread of data obtained. It is believed that the data spread is indicative of the three possible pathways (n = 0, 1 or 2) elucidated in Figure 8, which might be utilized in countless combinations and permutations by the 10^{10} - 10^{11} individual yeast cells present in the MFC. No *Pasteur Effect* [19], the acceleration of metabolic rate during fermentation, was observed with yeast under NR mediation which might have increased the power by 3 to 4 times. Also since the concentration of sugar used in these experiments was low, no "Crabtree effect" was observed either.

Clearly, MB was superior to NR when used as the sole mediator. The data was highly repeatable and showed power-density levels approximately four times that observed with NR. These results support the general hypothesis that MB promotes anaerobic respiration, whereas NR is associated with fermentation only in yeast.

When MB and NR were mixed, the affect on the MFC performance was dramatic, even though the overall mediator concentration remained unaltered. The peak power-density (0.52 W/m^2) was 25% higher than with MB alone, and was very consistent and repeatable. This result was consistent with the hypothesis presented in Figure 10, although more detailed stoichiometic measurements will be needed for precise confirmation.

In terms of peak power density the three cases of 1 mM NR, 1 mM MB, and ½ mM NR mixed with ½ mM MB were in the ratio 15:69:84 respectively, which was very close to the ratio of predicted energy efficiencies of 15:65:87.

Chapter 5 – Comparison of Different Electrodes

Clearly, the performance of MFCs is intrinsically related to the electrode materials. The electrodes for the present work were cut from reticulated vitreous carbon (RVC) foam, of 100 pores per inch. This material can be somewhat inconsistent in its manufacturing. Upon observation, the pores in the middle appeared darker and seemed to be denser.

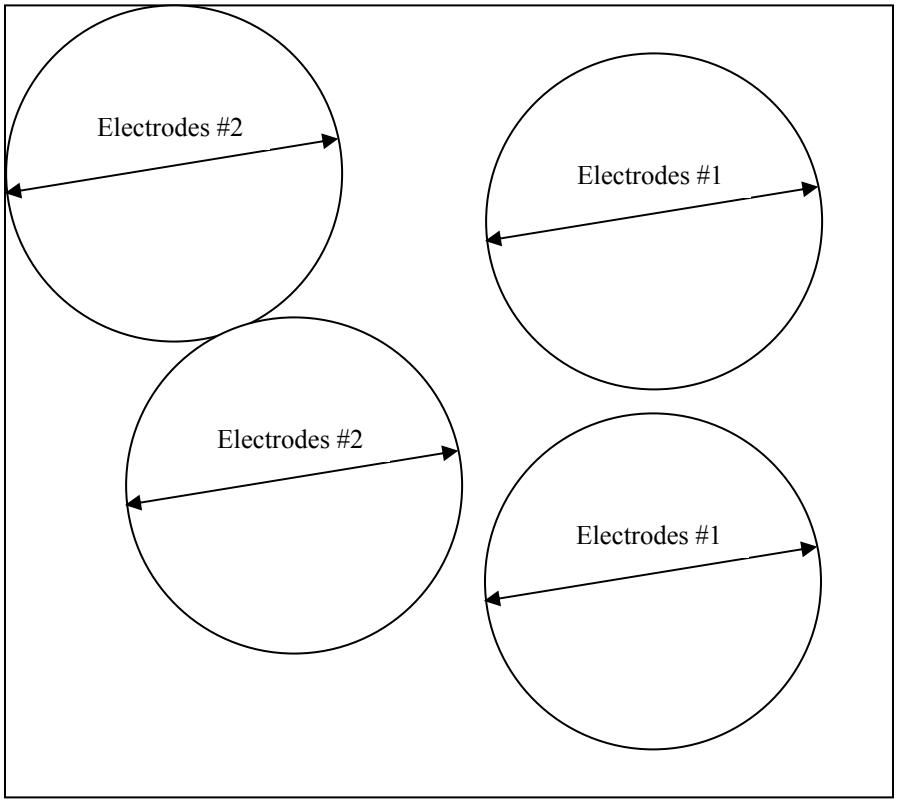

Figure 21: Location Where Electrodes Were Cut from Piece of RVC Foam Plate.

To study the variability of RVC electrodes, two sets (anode and cathode) were cut from the same piece of material. The electrodes for the first set (labeled as electrodes #1) were cut close to the middle of the sheet, whereas, the second set (labeled as electrodes #2) were cut closer to the corners of the sheet. It might be expected that all electrodes, cut the same way from the same piece of material, would perform the same, but this proved not to be the case.

Figure 27, in Appendix B, shows MFC performance using the two sets of RVC electrodes. Clearly, the Electrodes #1 showed substantially superior performance in comparison to the Electrodes #2.

In order to discover why the two sets of electrodes performed so differently, their conductivity was measured with an ohmmeter. It was found that the resistance was 2 kΩ/inch for the Electrodes #2 and 200 Ω/inch for Electrodes #1. Thus, a factor of 10 times in resistance was observed from the same piece of RVC material. This substantial difference could confirm why the peak power was so different between the two sets of electrodes.

Based on the results of these electrode tests, it was Electrodes #1 that were employed for the mediator test results reported in Figure 20.

Chapter 6 – Yeast Staining Phenomena

Mediator dyes are able to penetrate the outer cell lipid membranes and plasma wall of the yeast even though the yeast is so tiny, taking up a volume of less than 50 μm^3. Inside, the mediator interacts with the metabolic pathway, accepting electrons from co-enzyme intermediates, or acting as a surrogate terminal electron acceptor in the absence of oxygen [3]. In the latter case the process is more of an anaerobic respiration, rather than a traditional fermentation. Upon leaving the living cell the mediator becomes re-oxidized at the anode, thereby providing a circulatory electron transport coupling mechanism [3].

Yeast cells have distinguishable features, or organelles, within the cell that behave like our organs. Organelles do different tasks, some break down food into required nutrients for use in their normal activities. Past research has shown that some organalles of yeast are affected by mediator dyes more than others. Tests using fluorochromic dyes show that particular dyes affect some inclusion bodies more than others, if not exclusively [20]. With 1,000-fold magnification it is possible to examine yeast vacuole and cytosolic inclusion bodies to see how fluorchormic dyes affect them [20]. Individual cells from a particular yeast strain of a single species can display morphological and color heterogeneity [20].

On the macromolecular level, the body of yeast comprises proteins, glycoproteins, polysaccharides, polyphosphates, lipids, and nucleic acids [20]. These constituents attract

these dyes and the dyes act in place of an enzyme when breaking molecules down in order to obtain ATP energy.

From Table 2, it can be seen that Neutral Red Dye interacts with the Vacuoles only whereas Methylene Blue interacts within the whole cell. This specificity of NR to the vacuoles of yeast may partly explain the rather poor performance observed with this mediator in the MFC. NR is known to perform much better with *e-coli*, probably because NR acts more generally in this bacterium.

Table 2: Structure-specific Dyes for Yeast Cells [20].

Dye	Structures visualized	Comments
Methylene Blue	Whole cell	Non-viable cells stain blue
Aminoacidine	Cell walls	Indicator of surface potential
F-C ConA	Cell walls	Binds specifically to mannan
Calcofluor white	Bud scars	Chitin in scar fluoresces
DAPI(4,6-diamidino-2-phenylindole)	Nuclei	DNA fluoresces
Neutral Red	Vacuoles	Vacuoles stain red-purple
Iodine	Glycogen deposits	Glycogen stained red-brown
DAPI	Mitochondria	Mitochondria fluoresce pink-white
Rhodamine	Mitochondria	

Unlike NR, MB is able to pass through the membrane of yeast and all other inclusion bodies of the whole cell. This suggests that MB works with all parts of the yeast cell acting as an enzyme substitute in many different locations of the TCA cycle, see Figure 6.

Chapter 7 – Hydrogen Peroxide

A study on comparing different cathode oxidants was also performed, see Figure 29 in Appendix B. Some past researchers have chosen Hydrogen Peroxide as the catholyte based on its ability to accept ions and electrons. Hydrogen Peroxide (H_2O_2) combined with Hydrogen ions and electrons become water (H_2O), which has a very low energy state.

Using Hydrogen Peroxide in a MFC the cathodic reaction would become:

$$H_2O_2 + 2\ H^+ + 2\ e^- \rightarrow 2\ H_2O$$

The cathode redox potential in this case is +0.82 V compared to +0.36 V for Ferricyanide, which would inevitably lead to a larger OCV for the MFC.

A test using a 1mM concentration of Methylene Blue in the anolyte was used to compare Hydrogen Peroxide to Ferricyanide. As expected the open circuit potential was greater when using the Hydrogen Peroxide, see Figure 34 in Appendix C. Hydrogen Peroxide's main drawback was that its power dropped off much quicker than during the Ferricyanide tests. This is because the above cathodic reaction requires a catalyst to proceed at acceptable speed. A noble metal such as platinum is required as the catalyst, which is expensive and still requires elevated temperatures. So to maximize power density, ferricyanide instead of Hydrogen Peroxide was used for the entire test program reported here.

Ferricyanide also accepts electrons easily but its chemical kinetics are very fast. The cathodic reaction with ferricyanide is:

$$Fe(CN)_6^{3-} + H^+ + e^- \rightarrow Fe(CN)_6^{-4} + H^+$$

The drawback of ferricyanide is that the cathode reaction does not sweep up hydrogen ions (H^+) such that the buffer soon becomes exhausted with tan associated rise in pH.

Chapter 8 – Conclusion

Mediatorless biofuel cells are certainly desirable for a number of reasons (lower cost, flow-through design), but the output power possible from such systems is inevitably rather low. Although certain ion-reducing bacteria can transfer electrons directly to an anode, they do this via an outer membrane cytochrome-c of relatively high redox potential (+0.2 V). Because cytochrome-c (an electron carrier) is located towards the end of the transport chain the ion-reducing bacteria utilize approximately half of the fuel energy in ATP production. This results in an overall energy-efficiency significantly less than the 87% possible with targeted mediators, as shown in the formulation on page 18.

Despite the rather narrow approach adopted for predicting performance, the results obtained from the experimental yeast-catalyzed MFC mirrored these expectations quite closely in terms of relative power-density. In terms of peak power density, the three cases of 1 mM NR, 1 mM MB, and ½ mM NR mixed with ½ mM MB were in the ratio 15:69:84 respectively, shown in Figure 22. This experimental data was very close to the ratio of predicted energy efficiencies of 15:65:87 calculated on page 15, 17, and 18 respectively. The superior performance reported [13] for *e.coli* with NR alone was neither predicted nor observed with yeast. This is most likely due to the significant differences in fermentative pathways adopted by the two organisms. In addition, the mitochondrial physiology of yeast may impede trans-cellular passage of certain

mediators. For example, it is well known that MB is able to stain yeast whole-cells, while NR exclusively stains the vacuoles. It is plausible that such dye specificity to certain physiological structures may impact their effectiveness as mediators. For power-density, a combination of mediators was best suited. The high energy efficiency and improved power density of mixed-mediated MFCs makes them an attractive alternative to direct-exchange designs. However, mediated systems are currently best suited to "bio-battery" applications where mediators are not lost via the waste stream of "flow-through" biofuel cell configurations. Immobilization or mediator separation/recycling techniques may eventually remove this limitation.

Future research is required to study mediator ratios other than 50% NR + 50% MB, such as 20% NR + 80% MB etc., in order to find the optimum mix ratio. In addition the experiments need to be repeated with an oxygen cathode using Platinum as a cathodic catalyst.

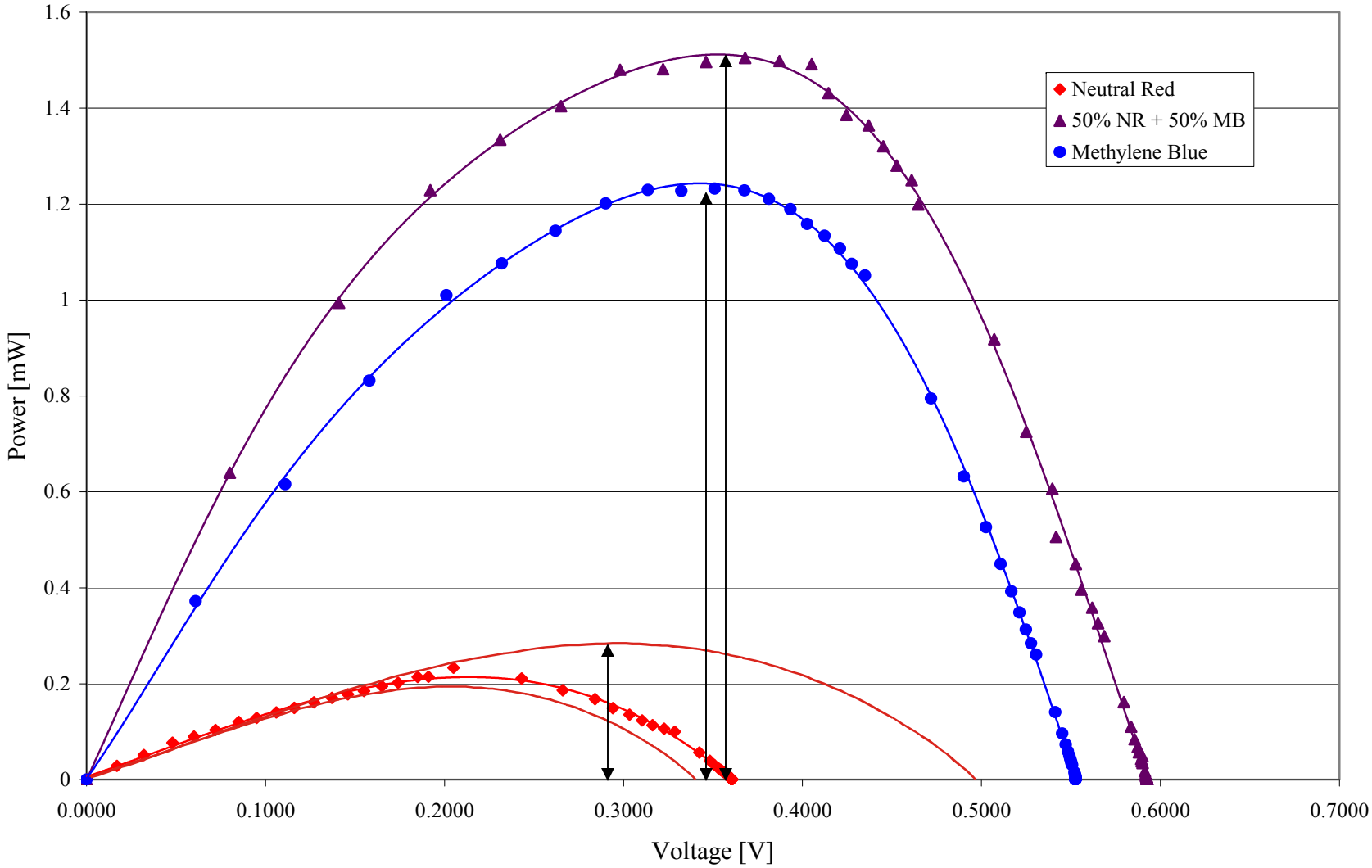

Figure 22: Comparison of Peak Power.

References

[1] Lewis, Nancy D. http://itp.nyu.edu/~nql3186/electricity/timeline.html#Volta Accessed: November 2005.

[2] Wilkinson, S., "Gastrobots – Benefits and Challenges of Microbial Fuel Cells in Food Powered Robot Applications", J. Autonomous Robots, 9(2), September, 2000, pp. 99-111.

[3] Wilkinson, S., ""Juice from Juice" – Electricity Generation for Carpophagous Gastrobots", IASTED 2000 Int. Conf. On Robotics & Applications, Clearwater, Florida, Nov. 19-22, 2001, paper #246-036.

[4] Wilkinson, S., "Gastronome – A Pioneering Food Powered Mobile Robot", Proc. IASTED 2000 (8th) Int. Conf. On Robotics & Applications, Honolulu, Hawaii, Aug. 14-16, 2000, pp. 176-181.

[5] Bennetto, H.P., "Electricity Generation by Microorganisms", *Biotechnology Education*, Vol. 1, No. 4, Column 3, 1990, p. 164.

[6] Bennetto, H.P., Dew, M.E., Stirling, J.L., and Tanaka, K., "Rates of Reduction of Phenothiazine Redox Dyes by *E. col*i", *Chemistry and Industr*y, 1981, pp. 776–778.

[7] Delaney, G.M., Bennetto, H.P., Mason, J.R., Roller, H.D., Stirling, J.L., and Thurston, C.F., "Electron-transfer Coupling in Microbial Fuel Cells: 2. Performance of Fuel Cells Containing Selected Micoorganism-Mediator-Substrate Combinations", *J. Chem.Tech. Biotechnol*., 34B, 1984, pp.13–27.

[8] Bennetto, H.P., "Microbial Fuel Cells", Life Chemistry Reports, Harwood Academic Publishers GmbH and OPA Ltd, Vol. 2, No. 4., 1984, pp. 371-373.

[9] Lithgow, A.M., Romero, L., Sanchez, I.C., Souto, F.A., and Vega, C.A., "Interception of Electron-transport Chain in Bacteria with Hydrophilic Redox Mediators", *J. Chem. Res.*, (S), 1986, pp. 178–179.

[10] Tanaka, K., Vega, C.A., and Tamamushi, R., "Thionine and Ferric Chelate Compounds as Coupled Mediators in Microbial Fuel Cells", *Bioelectricity and Bioenergetic*s, 11, 1983, pp. 289–297.

[11] Bennetto, H.P., Stirling, J.L., Tanaka, K., Vega, C.A., *Soc. Gen. Microb. Quart.,* Vol. 8, No. 1, 1980, p. 37; "Anodic Reactions in Microbial Fuel Cells" *Biotechnol. Bioeng.*, Vol. 25, 1983, pp. 559-568.

[12] Zhang, X. and Halme, A., "A Summary of the Study of Bio-electrochemical Fuel Cell by Using *Saccharomyces cerevisiae*", Research Reports of Automation Technology Laboratory of HUT, No. 10, January, 1994.

[13] Park, D.H. and Zeikus, J.G., "Electricity Generation in Microbial Fuel Cells Using Neutral Red as an Electronophore", *Appl. Environ. Microbiol.*, 66, 2000, pp. 1292-1297.

[14] Clark, W.M., Oxidation-Reduction Potentials of Organic Systems, Williams & Wilkins, Baltimore, 1960, pp. 125, 131, 132, 415 and 496.

[15] Park, D.H. and Zeikus, J.G., "Utilization of Electrically Reduced Neutral Red by Actinobacillus succinogenes: Physiological Function of Neutral Red in Membrane-Driven Fumarate Reduction and Energy Conservation", *J. Bacteriology*, Vol. 181, No. 8, April 1999, pp. 2403-2410.

[16] Thunberg, T., "Das Reduktions-Oxydationspotential eines Gemisches von Succinat-Fumerat", *Skand. Arch. Physiol*., Vol. 46, 1925, pp. 339.

[17] Quastel, J.H. and Whetham, M.D., "The Equilibria Existing Between Succinic, Fumaric and Malic Acids in the Presence of Resting Bacteria", B*iochem. J*., Vol. 18, 1924, p. 519.

[18] Thurston, C.F., Bennetto, H.P., Delaney, G.M., Mason, J.R., Roller, H.D., and Stirling, J.L., "Glucose Metabolism in a Microbial Fuel Cell - Stoichiometry of Product Formation in a Thionine-mediated *Proteus vulgaris* Fuel Cell and its Relation to Coulombic Yields", *Journal of General Microbiology*, 131, 1985, pp. 1393–1401.

[19] Gottschalk, G., Bacterial Metabolism, 2nd Edition, Springer-Verlag, Ch. 8., Section IB, 1986, p. 213.

[20] Feldman, H., Yeast Cell Architecture and Function, Butendadt – Institute, University of Munich, 2005, http://biochemie.web.med.uni-muenchen.de/Yeast_Biol/ Accessed: December 2005.

Bibliography

Bungay, Rensselaer Polytechnical Institute.
http://www.rpi.edu/dept/chem-eng/Biotech-Environ/Contin/overload.html

Dickinson, J.R. and Schweizer, M., eds., "The Metabolism and Molecular Physiology of *Saccharomyces cerevisiae*", Taylor & Francis, London/Philadelphia, 1999.

Moller, P., Electric Fishes: History and Behavior, Fish and Fisheries Series 17, Chapman & Hall.NY, 1995.

Wilkinson, S. and Guanio, D., "Development of a Spectrometric Citrus Odor Sensor for a Frugivorous Robot", Proc. 6th IASTED Int. Conf. Robotics & Manufacturing, paper 284-014, Banff, Canada, July 26-29, 1998, pp. 252-255.

Appendices

Appendix A: Tabulated Experimental Results

Table 3: Experimental Results for NR Only Electrodes #2.

Resistance Ω	Volts V	Power mW	Current Amp	LOG(I) Amp	Resistance Ω	Volts V	Power mW	Current Amp	LOG(I) Amp
1000080	0.3603	0.0001	3.60E-07	-6.4434	1080	0.3286	0.1000	3.04E-04	-3.5168
900080	0.3603	0.0001	4.00E-07	-6.3976	980	0.3227	0.1063	3.29E-04	-3.4824
800080	0.3604	0.0002	4.50E-07	-6.3463	880	0.3162	0.1136	3.59E-04	-3.4445
700080	0.3603	0.0002	5.15E-07	-6.2885	780	0.3103	0.1234	3.98E-04	-3.4003
600080	0.3604	0.0002	6.01E-07	-6.2214	680	0.3034	0.1354	4.46E-04	-3.3505
500080	0.3605	0.0003	7.21E-07	-6.1421	580	0.2940	0.1490	3.04E-04	-6.4434
400080	0.3605	0.0003	9.01E-07	-6.0452	480	0.2840	0.1680	3.04E-04	-6.4434
300080	0.3606	0.0004	1.20E-06	-5.9202	380	0.2660	0.1862	3.04E-04	-6.4434
200080	0.3605	0.0006	1.80E-06	-5.7443	280	0.2430	0.2109	3.04E-04	-6.4434
100080	0.3603	0.0013	3.60E-06	-5.4437	180	0.2050	0.2335	3.04E-04	-6.4434
90080	0.3603	0.0014	4.00E-06	-5.3980	170	0.1910	0.2146	3.04E-04	-6.4434
80080	0.3602	0.0016	4.50E-06	-5.3470	160	0.1850	0.2139	3.04E-04	-6.4434
70080	0.3602	0.0019	5.14E-06	-5.2891	150	0.1740	0.2018	3.04E-04	-6.4434
60080	0.3601	0.0022	5.99E-06	-5.2223	140	0.1650	0.1945	3.04E-04	-6.4434
50080	0.3601	0.0026	7.19E-06	-5.1432	130	0.1550	0.1848	3.04E-04	-6.4434
40080	0.3599	0.0032	8.98E-06	-5.0467	120	0.1460	0.1776	3.04E-04	-6.4434
30080	0.3596	0.0043	1.20E-05	-4.9225	110	0.1370	0.1706	3.04E-04	-6.4434
20080	0.3591	0.0064	1.79E-05	-4.7475	100	0.1270	0.1613	3.04E-04	-6.4434
10080	0.3575	0.0127	3.55E-05	-4.4502	90	0.1160	0.1495	3.04E-04	-6.4434
9080	0.3567	0.0140	3.93E-05	-4.4058	80	0.1060	0.1405	3.04E-04	-6.4434
8080	0.3560	0.0157	4.41E-05	-4.3560	70	0.0950	0.1289	3.04E-04	-6.4434
7080	0.3552	0.0178	5.02E-05	-4.2996	60	0.0850	0.1204	3.04E-04	-6.4434
6080	0.3542	0.0206	5.83E-05	-4.2347	50	0.0720	0.1037	3.04E-04	-6.4434
5080	0.3528	0.0245	6.94E-05	-4.1583	40	0.0600	0.0900	3.04E-04	-6.4434
4080	0.3508	0.0302	8.60E-05	-4.0656	30	0.0480	0.0768	3.04E-04	-6.4434
3080	0.3482	0.0394	1.13E-04	-3.9467	20	0.0320	0.0512	3.04E-04	-6.4434
2080	0.3424	0.0564	1.65E-04	-3.7835	10	0.0170	0.0289	3.04E-04	-6.4434

Appendix A: (continued)

Table 4: Experimental Results for NR and MB Electrodes # 2.

Resistance [Ω]	Volts [V]	Power [mW]	Current [Amp]	LOG(I)	Resistance [Ω]	Volts [V]	Power [mW]	Current [Amp]	LOG(I)
1,000,080	0.5922	0.0004	5.92E-07	-6.2276	1,080	0.5449	0.2749	5.05E-04	-3.2971
900,080	0.5921	0.0004	6.58E-07	-6.1819	980	0.5385	0.2959	5.49E-04	-3.2600
800,080	0.5921	0.0004	7.40E-07	-6.1307	880	0.5321	0.3217	6.05E-04	-3.2185
700,080	0.5921	0.0005	8.46E-07	-6.0728	780	0.5245	0.3527	6.72E-04	-3.1723
600,080	0.5921	0.0006	9.87E-07	-6.0058	680	0.5150	0.3900	7.57E-04	-3.1207
500,080	0.5921	0.0007	1.18E-06	-5.9266	580	0.5035	0.4371	8.68E-04	-3.0614
400,080	0.5921	0.0009	1.48E-06	-5.8298	480	0.4891	0.4984	1.02E-03	-2.9918
300,080	0.5920	0.0012	1.97E-06	-5.7049	380	0.4703	0.5821	1.24E-03	-2.9074
200,080	0.5919	0.0018	2.96E-06	-5.5290	280	0.4341	0.6730	1.55E-03	-2.8096
100,080	0.5916	0.0035	5.91E-06	-5.2283	180	0.3764	0.7871	2.09E-03	-2.6796
90,080	0.5915	0.0039	6.57E-06	-5.1827	170	0.3649	0.7832	2.15E-03	-2.6683
80,080	0.5914	0.0044	7.39E-06	-5.1316	160	0.3538	0.7823	2.21E-03	-2.6554
70,080	0.5913	0.0050	8.44E-06	-5.0738	150	0.3431	0.7848	2.29E-03	-2.6407
60,080	0.5912	0.0058	9.84E-06	-5.0070	140	0.3316	0.7854	2.37E-03	-2.6255
50,080	0.5910	0.0070	1.18E-05	-4.9281	130	0.3190	0.7828	2.45E-03	-2.6102
40,080	0.5907	0.0087	1.47E-05	-4.8316	120	0.3065	0.7829	2.55E-03	-2.5928
30,080	0.5902	0.0116	1.96E-05	-4.7073	110	0.2950	0.7911	2.68E-03	-2.5716
20,080	0.5900	0.0173	2.94E-05	-4.5319	100	0.2770	0.7673	2.77E-03	-2.5575
10,080	0.5867	0.0341	5.82E-05	-4.2350	90	0.2610	0.7569	2.90E-03	-2.5376
9,080	0.5859	0.0378	6.45E-05	-4.1903	80	0.2410	0.7260	3.01E-03	-2.5211
8,080	0.5850	0.0424	7.24E-05	-4.1403	70	0.2220	0.7041	3.17E-03	-2.4987
7,080	0.5841	0.0482	8.25E-05	-4.0835	60	0.2000	0.6667	3.33E-03	-2.4771
6,080	0.5825	0.0558	9.58E-05	-4.0186	50	0.1750	0.6125	3.50E-03	-2.4559
5,080	0.5807	0.0664	1.14E-04	-3.9419	40	0.1460	0.5329	3.65E-03	-2.4377
4,080	0.5780	0.0819	1.42E-04	-3.8487	30	0.1150	0.4408	3.83E-03	-2.4164
3,080	0.5740	0.1070	1.86E-04	-3.7296	20	0.0790	0.3121	3.95E-03	-2.4034
2,080	0.5659	0.1540	2.72E-04	-3.5653	10	0.0410	0.1681	4.10E-03	-2.3872

Appendix A: (continued)

Table 5: Experimental Results for MB Only Electrodes #2.

Resistance Ω	Volts V	Power mW	Current Amp	LOG(I) Amp	Resistance Ω	Volts V	Power mW	Current Amp	LOG(I) Amp
1000080	0.5524	0.0003	5.52E-07	-6.2578	1080	0.5306	0.2607	4.91E-04	-3.3087
900080	0.5525	0.0003	6.14E-07	-6.2119	980	0.5277	0.2842	5.38E-04	-3.2688
800080	0.5525	0.0004	6.91E-07	-6.1608	880	0.5248	0.3130	5.96E-04	-3.2245
700080	0.5525	0.0004	7.89E-07	-6.1028	780	0.5212	0.3483	6.68E-04	-3.1751
600080	0.5526	0.0005	9.21E-07	-6.0358	680	0.5167	0.3926	7.60E-04	-3.1193
500080	0.5526	0.0006	1.11E-06	-5.9566	580	0.5107	0.4497	8.81E-04	-3.0553
400080	0.5527	0.0008	1.38E-06	-5.8597	480	0.5026	0.5263	1.05E-03	-2.9800
300080	0.5527	0.0010	1.84E-06	-5.7347	380	0.4901	0.6321	1.29E-03	-2.8895
200080	0.5527	0.0015	2.76E-06	-5.5587	280	0.4718	0.7950	1.69E-03	-2.7734
100080	0.5526	0.0031	5.52E-06	-5.2579	180	0.4350	1.0513	2.42E-03	-2.6168
90080	0.5526	0.0034	6.13E-06	-5.2122	170	0.4275	1.0750	2.51E-03	-2.5995
80080	0.5526	0.0038	6.90E-06	-5.1611	160	0.4209	1.1072	2.63E-03	-2.5799
70080	0.5526	0.0044	7.89E-06	-5.1032	150	0.4124	1.1338	2.75E-03	-2.5608
60080	0.5526	0.0051	9.20E-06	-5.0363	140	0.4027	1.1583	2.88E-03	-2.5411
50080	0.5526	0.0061	1.10E-05	-4.9573	130	0.3932	1.1893	3.02E-03	-2.5193
40080	0.5525	0.0076	1.38E-05	-4.8606	120	0.3812	1.2109	3.18E-03	-2.4980
30080	0.5523	0.0101	1.84E-05	-4.7361	110	0.3676	1.2285	3.34E-03	-2.4760
20080	0.5519	0.0152	2.75E-05	-4.5609	100	0.3510	1.2320	3.51E-03	-2.4547
10080	0.5507	0.0301	5.46E-05	-4.2625	90	0.3324	1.2277	3.69E-03	-2.4326
9080	0.5504	0.0334	6.06E-05	-4.2174	80	0.3136	1.2293	3.92E-03	-2.4067
8080	0.5501	0.0375	6.81E-05	-4.1670	70	0.2900	1.2014	4.14E-03	-2.3827
7080	0.5497	0.0427	7.76E-05	-4.1099	60	0.2620	1.1441	4.37E-03	-2.3598
6080	0.5491	0.0496	9.03E-05	-4.0443	50	0.2320	1.0765	4.64E-03	-2.3335
5080	0.5483	0.0592	1.08E-04	-3.9668	40	0.2010	1.0100	5.03E-03	-2.2989
4080	0.5471	0.0734	1.34E-04	-3.8726	30	0.1580	0.8321	5.27E-03	-2.2785
3080	0.5451	0.0965	1.77E-04	-3.7521	20	0.1110	0.6161	5.55E-03	-2.2557
2080	0.5412	0.1408	2.60E-04	-3.5847	10	0.0610	0.3721	6.10E-03	-2.2147

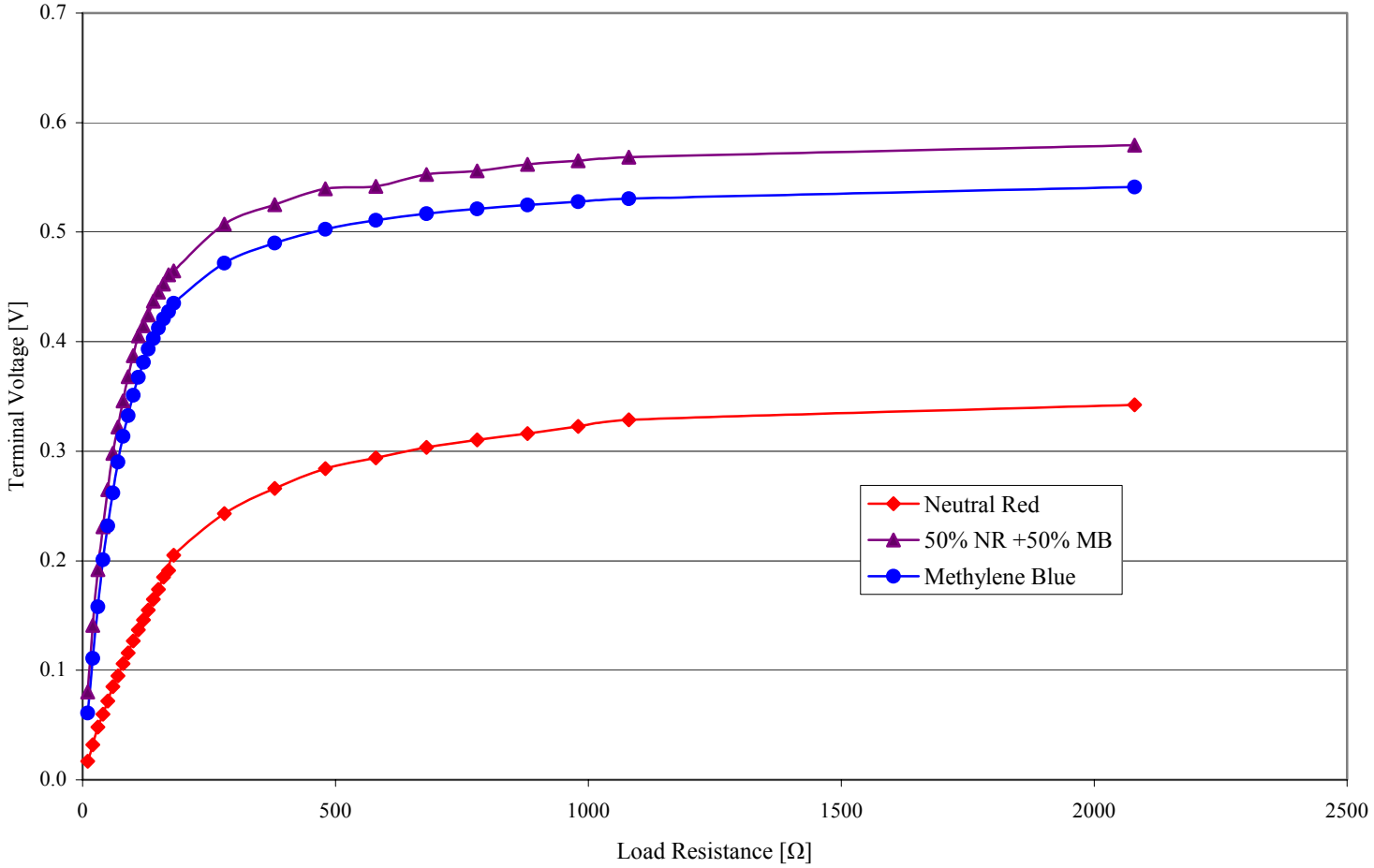

Figure 23: Voltage vs. Resistance.

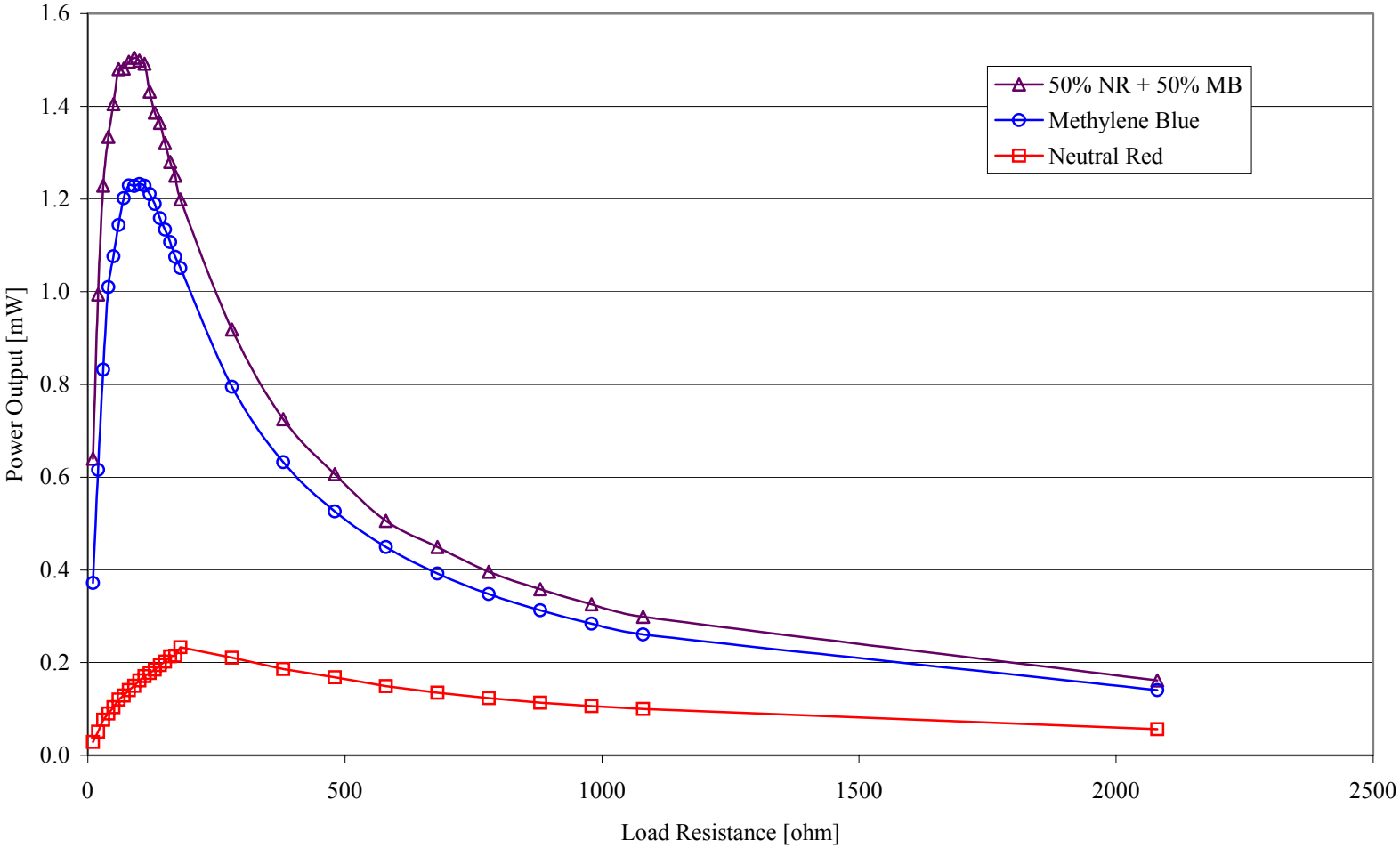

Figure 24: Power vs. Resistance.

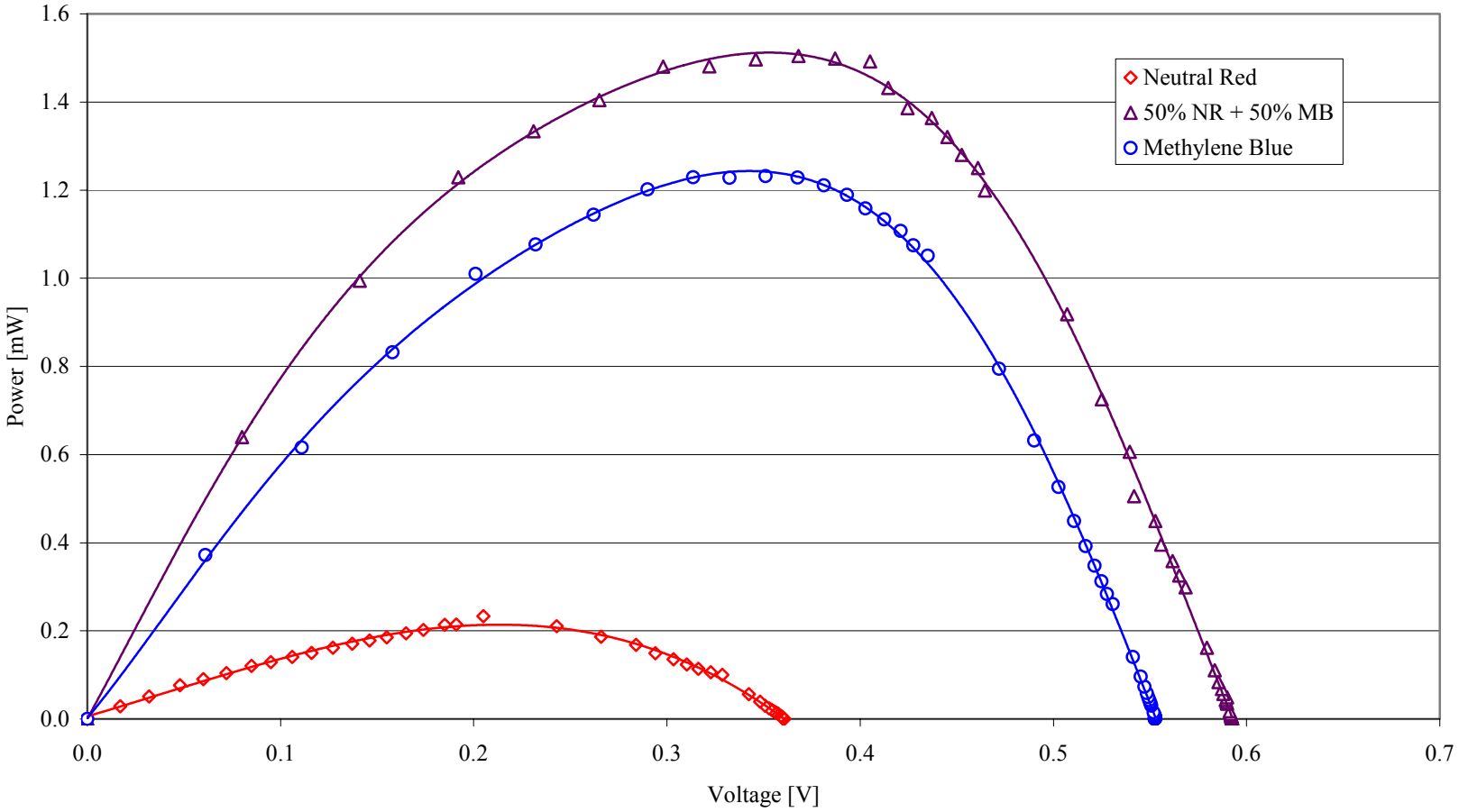

Figure 25: Power vs. Voltage.

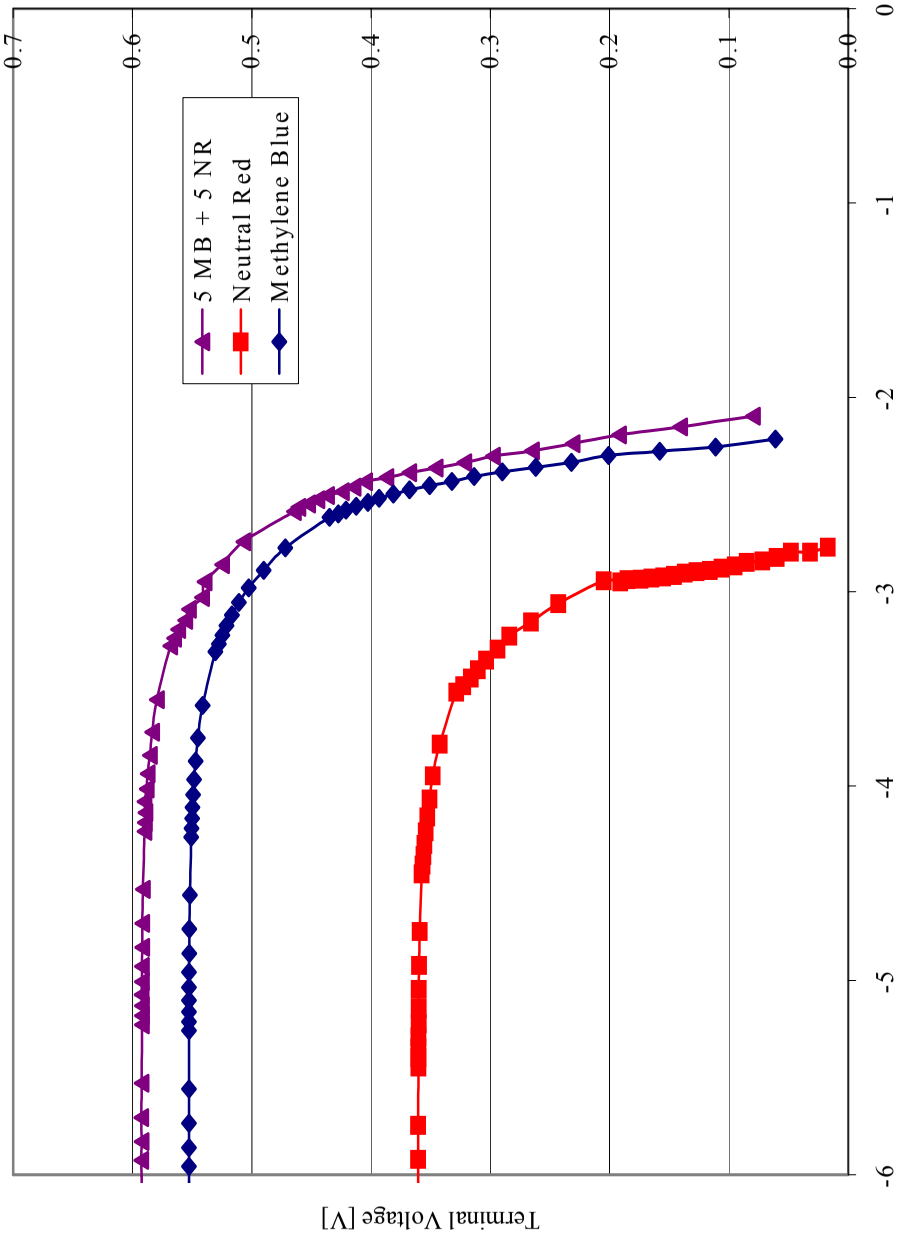

Figure 26: Log of Current vs. Voltage.

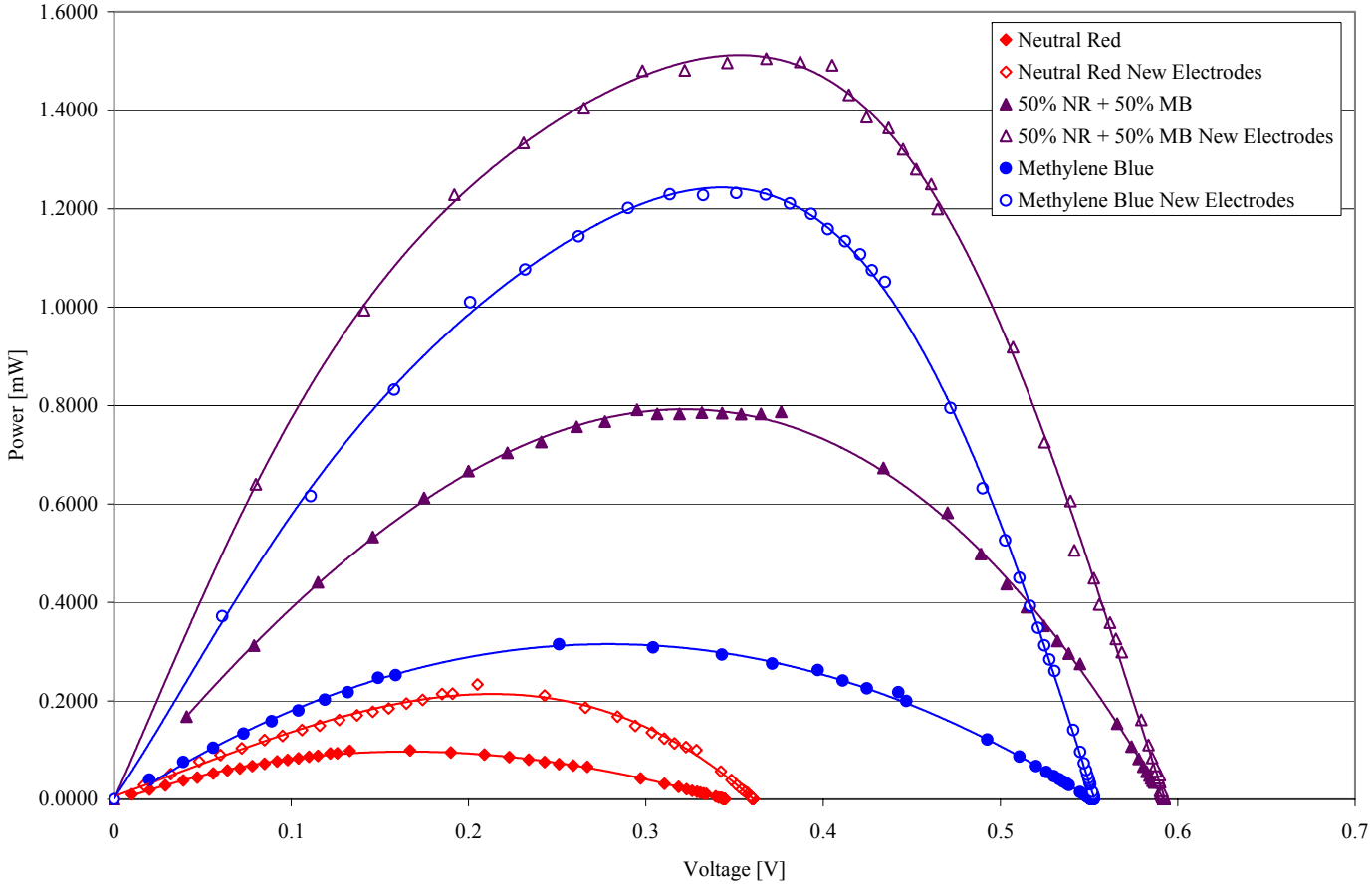

Figure 27: Power vs. Voltage for Different Electrodes.

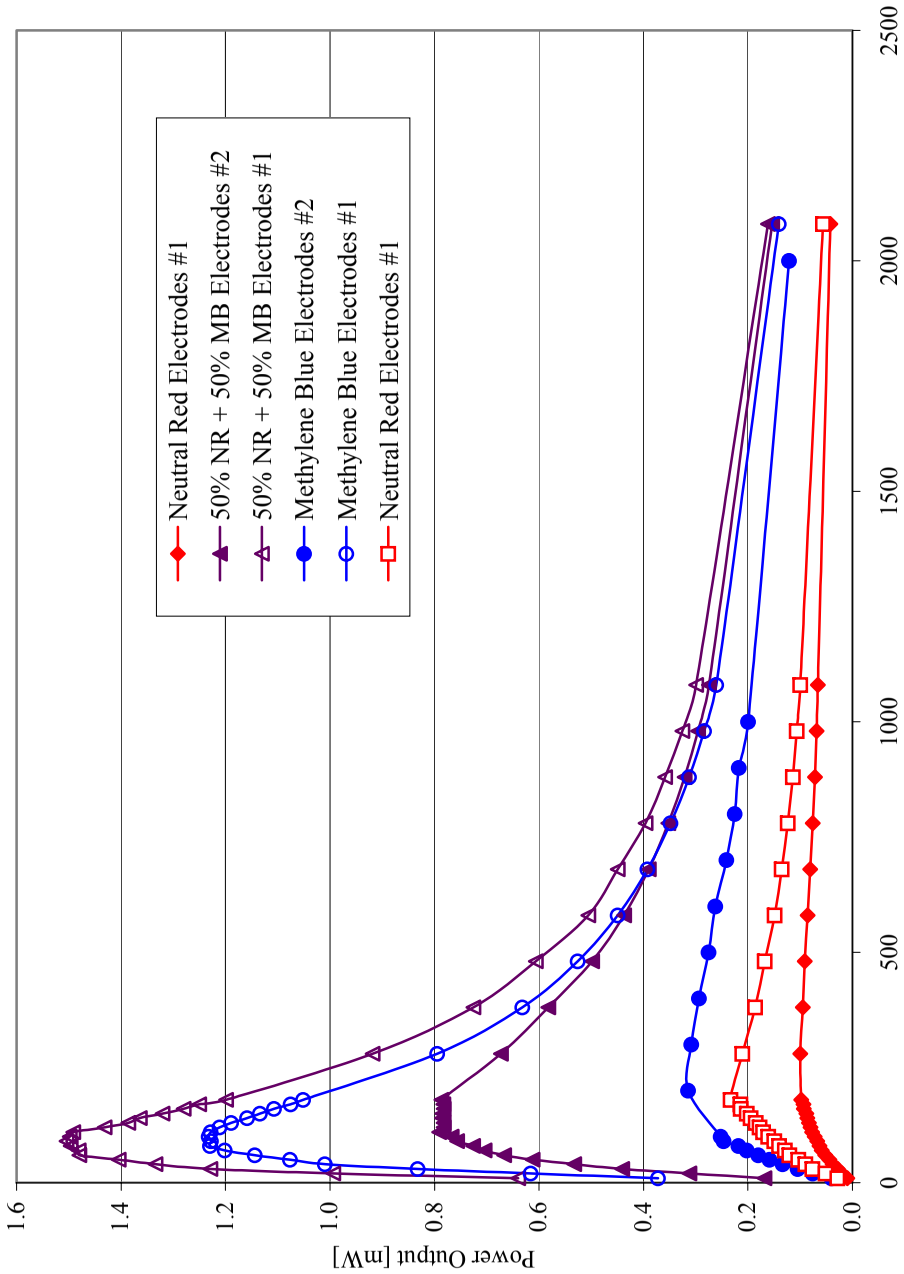

Figure 28: Power vs. Resistance for Different Electrodes.

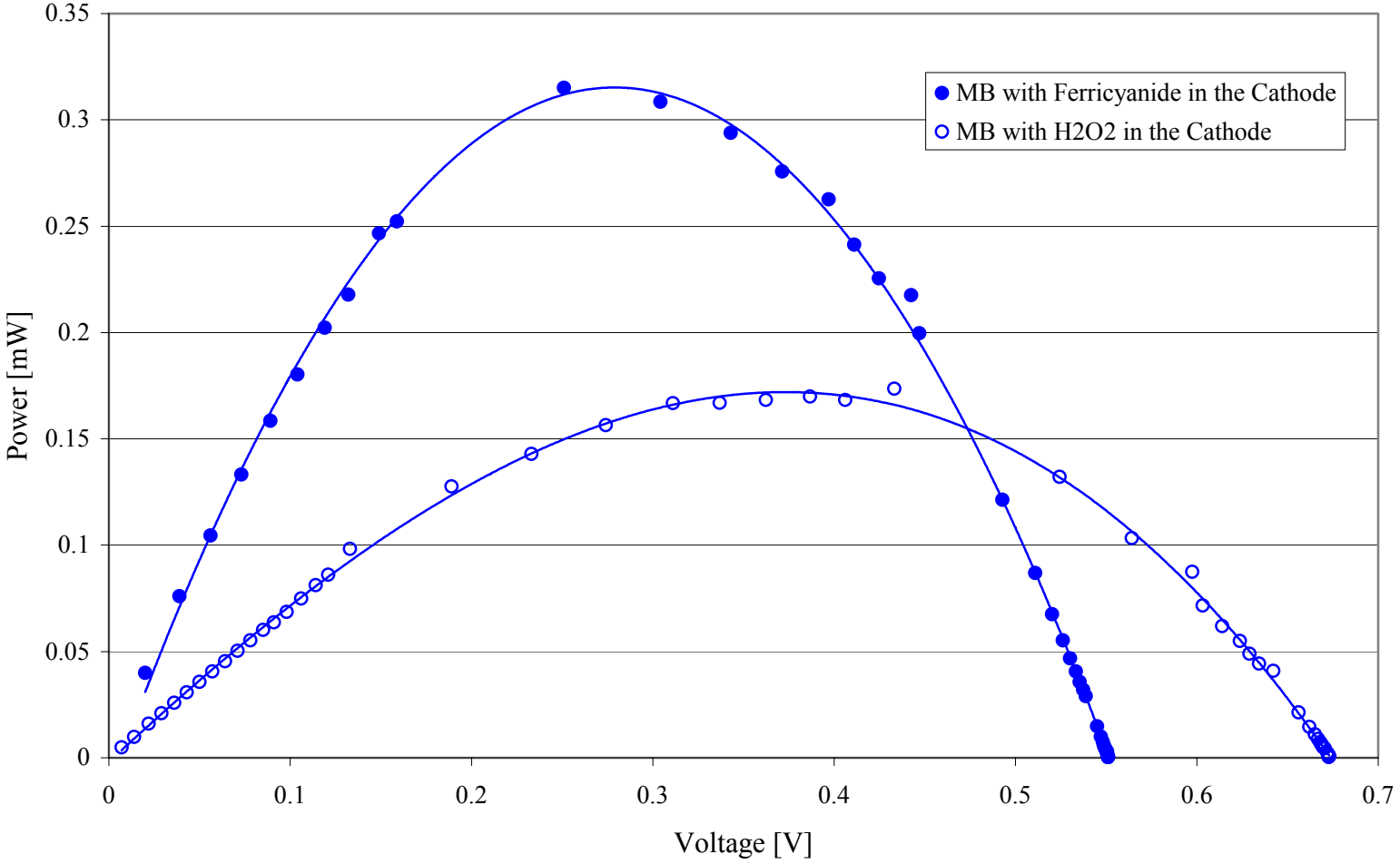

Figure 29: Comparison of Hydrogen Peroxide to Ferricyanide in the Cathode.

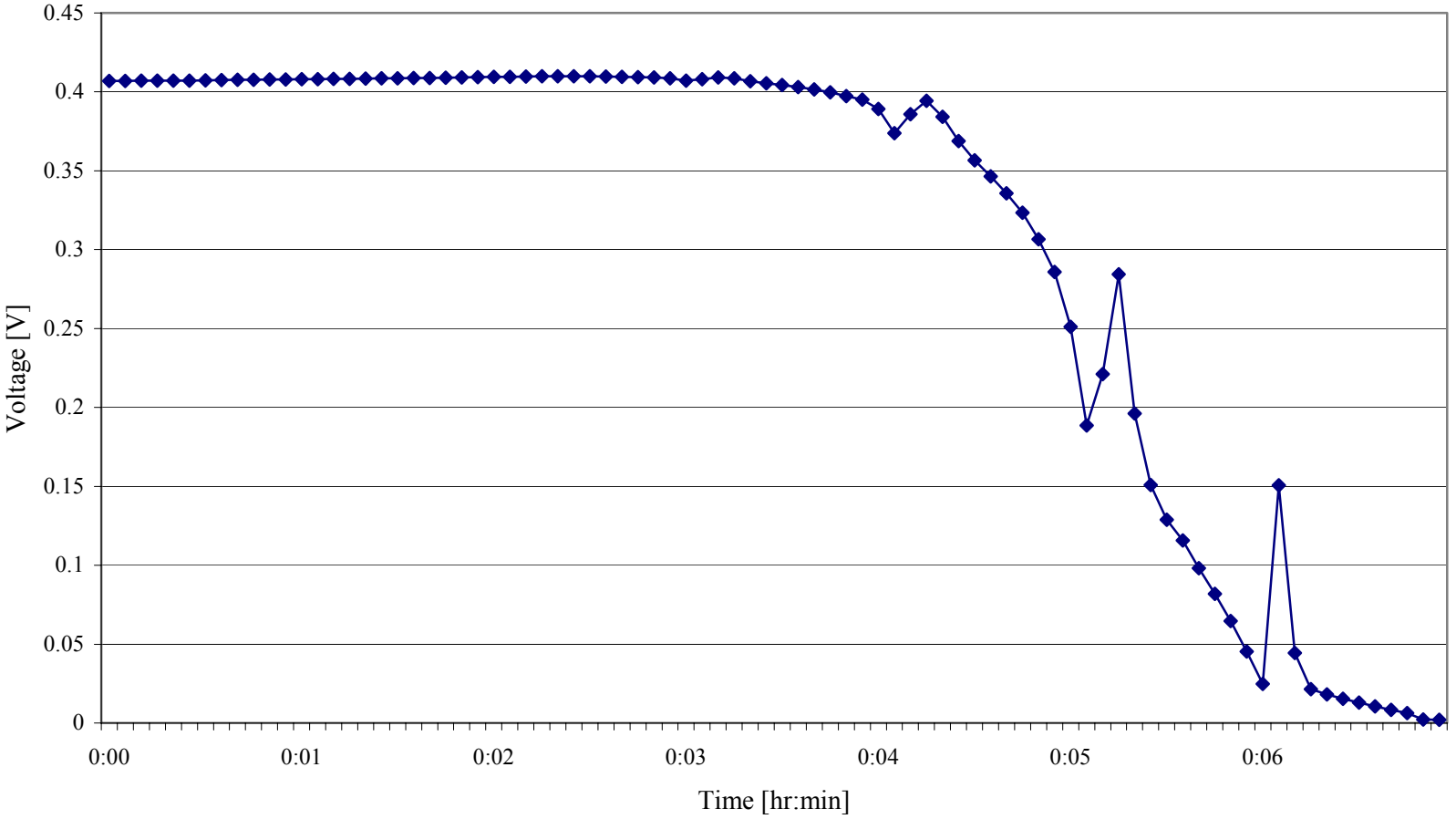

Figure 30: Fluke Data for No Mediator.

Appendix C: (Continued)

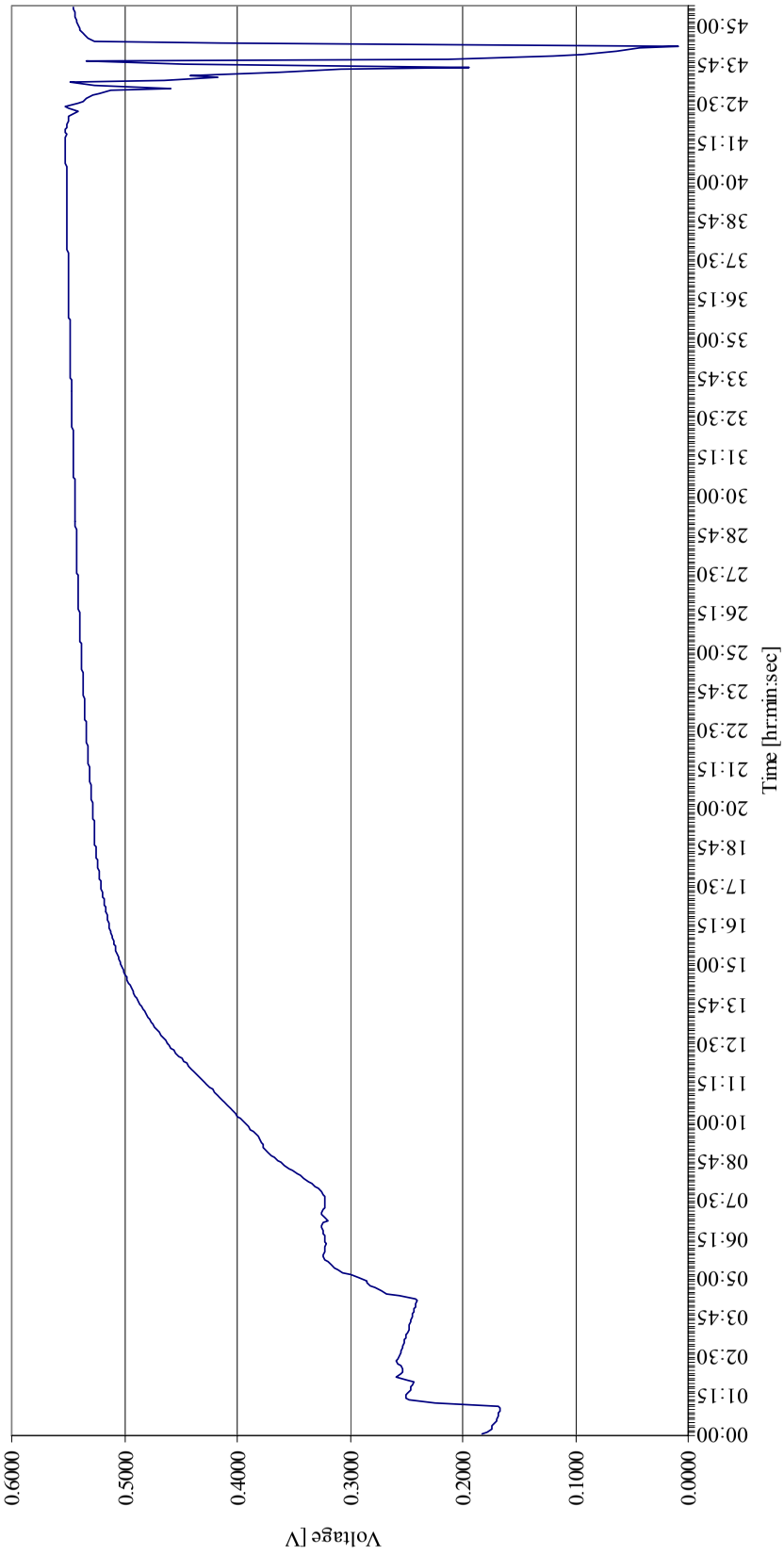

Figure 31: Fluke Data for MB.

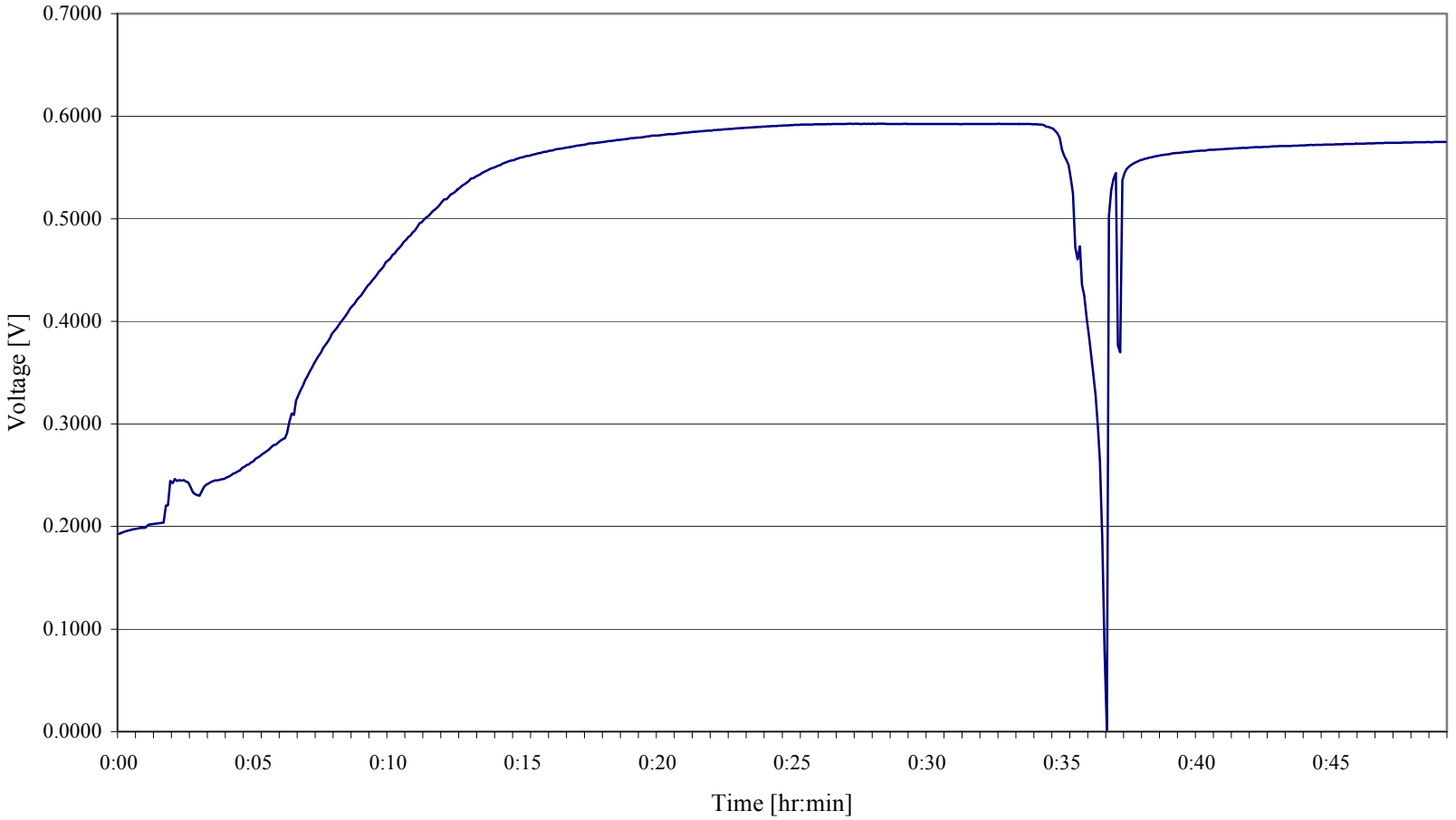

Figure 32: Fluke Data for MB and NR.

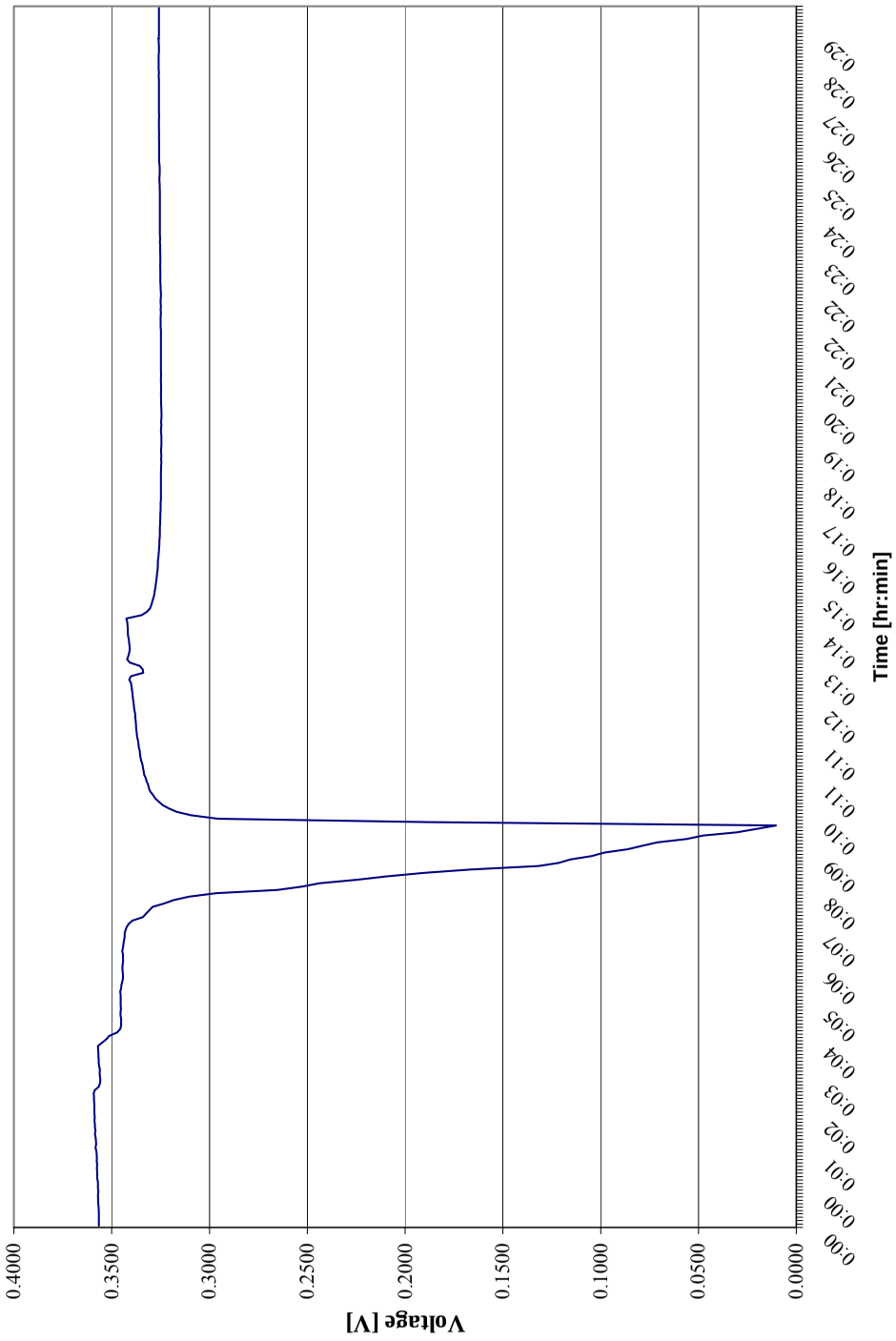

Figure 33: Fluke Data for NR.

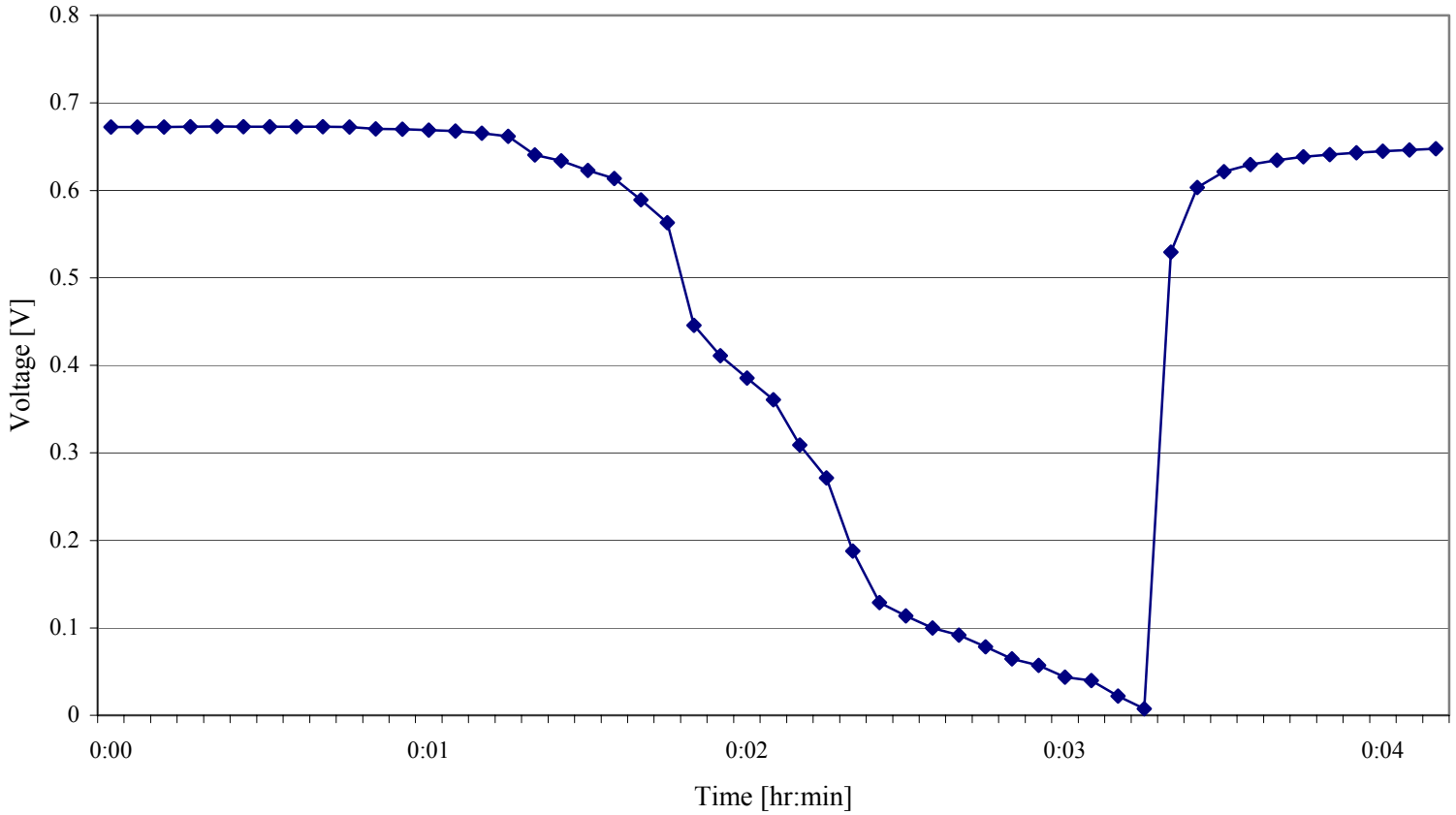

Figure 34: Fluke Data for MB With H_2O_2 in the Cathode.